Computers & Industrial Engineering 134 (2019) 11–26

Contents lists available at ScienceDirect

Computers & Industrial Engineering

journal homepage: www.elsevier.com/locate/caie

Real-time frequency regulation using aggregated electric vehicles in smart grid

Md. Monirul Islam[a], Xiao Zhong[a], Zeyi Sun[a,*], Haoyi Xiong[b,c], Wenqing Hu[d]

[a] Department of Engineering Management and Systems Engineering, Missouri University of Science and Technology, Rolla, MO 65409, United States
[b] Department of Computer and Information Science, University of Macau, Macau, China
[c] State Key Laboratory of Internet of Things for Smart City, University of Macau, Macau, China
[d] Department of Mathematics and Statistics, Missouri University of Science and Technology, Rolla, MO 65409, United States

ARTICLE INFO

Keywords:
Electric vehicle
Frequency regulation
Real-time
Smart grid

ABSTRACT

The electric vehicle (EV) market has witnessed a continuous and steady increase in the past few years. The benefits of lower energy costs and less greenhouse gas (GHG) emission have been widely recognized by customers. In addition to these benefits for the transportation sector, EVs are also considered a critical supplementary resource for building a sustainable energy system in a smart grid environment. The applications of EVs in a smart grid have attracted wide attention in recent years. One appealing application is to use aggregated EVs as either energy sources or sinks to provide a service of frequency regulation for the request signals from the grid. A real-time decision-making model is proposed in this paper for the EV aggregator to dynamically control the energy flow between the grid and each individual EV in the aggregated group as an effective response to the signals of frequency regulation issued by the grid using Markov Decision Process. The aggregator's benefit is maximized through the identification of a set of optimal charging/discharging decisions for the aggregated EVs. A semi-online solution strategy is also proposed to find the near-optimal decisions on a real-time basis. A numerical case study is used to illustrate the effectiveness of the proposed model.

1. Introduction

Due to the increasing concerns of climate change and environmental protection, the significance of sustainability awareness for integrated operations in various energy end-use sectors has been gradually recognized. In the residential sector, smart-living has been proposed to guide residential end-use customers to utilize resources and energy more efficiently (European Union, 2014). In the industrial sector, sustainability strategies have been widely adopted by many manufacturing end-use customers to balance the productivity and environment-related performance of industrial facilities. Many studies focusing on production decision-making for manufacturers have been reported. For example, Xia, Xi, Du, Xiao, and Pan (2017) proposed energy-oriented maintenance decision-making towards sustainable manufacturing. Li, Sun, Yang, and Gu (2012) developed a simulation-based optimal energy control model for manufacturing systems to reduce energy waste and improve energy efficiency. For more references in this area, the readers can check the literature (Duan, Deng, Gharaei, Wu, & Wang, 2018; Dubey, Gunasekaran, Sushil, & Singh, 2015; Hao, Helo, & Shamsuzzoha, 2018; Kazemi, Abdul-Rashid, Ghazilla, Shekarian, & Zanoni, 2018). Furthermore, carbon-constrained supply chain design and optimization for different industries have also been widely investigated. For example, Gharaei, Karimi, and Hoseini Shekarabi (2019a) proposed an integrated multi-product, multi-buyer supply chain under penalty, green, and quality control polices. More references in this topic are available in the literature (Gharaei, Hoseini Shekarabi, & Karimi, 2019; Gharaei, Karimi, and Hoseini Shekarabi, 2019b; Hoseini Shekarabi, Gharaei, & Karimi, 2018; Rabbani, Hosseini-Mokhallesun, Ordibazar, & Farrokhi-Asl, 2018; Rabbani, Foroozesh, Mousavi, & Farrokhi-Asl, 2019; Tsao, 2015).

In the transportation sector, environmentally friendly planning considering both cost and emissions has been investigated. For example, Sayyadi and Awasthi (2018a) presented an integrated approach based on system-dynamics simulations and analytic network processing to evaluate sustainable transportation policies that considered congestion level, fuel consumption, and emission. More references in the transportation sector are available in the literature (Awasthi & Omrani, 2019; Sayyadi & Awasthi, 2018b).

In addition, the technology of Electric Vehicles (EVs) is a promising alternative to the traditional combustion engine vehicle and has been

* Corresponding author.
E-mail address: sunze@mst.edu (Z. Sun).

https://doi.org/10.1016/j.cie.2019.05.025
Received 26 January 2018; Received in revised form 5 May 2019; Accepted 20 May 2019
Available online 21 May 2019
0360-8352/

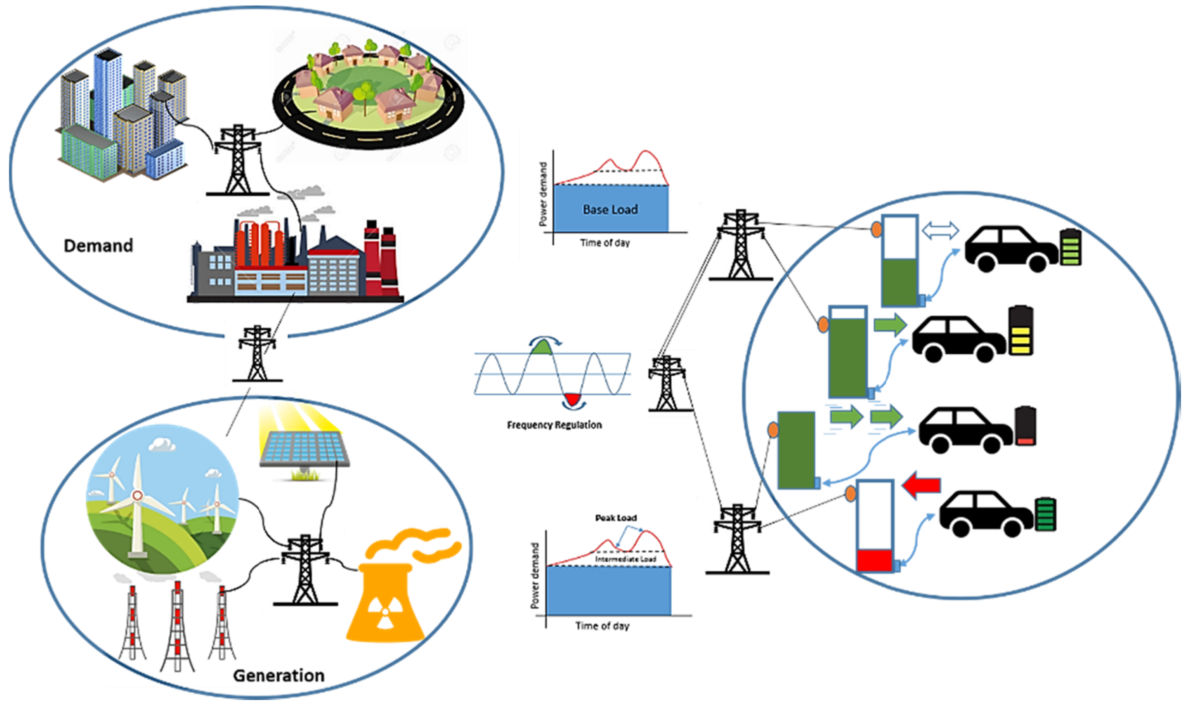

Fig. 1. EV's three integration modes into the grid.

frequently spotlighted in the transportation sector throughout the last decade. During the past few years, the global market share of EVs has been steadily rising, reaching a milestone of one million EV sales worldwide (Lutsey, 2015). The benefits of lower energy costs and less greenhouse gas (GHG) emission have been widely recognized by customers.

Using GHG emission reduction as an example, the incurred emissions in driving using EVs can be estimated as follows when assuming the electricity used to support EV driving is generated using coal. The electricity consumption of an EV for a 100-mile drive ranges from 25 to 36 kWh, depending on the make and model of the EV (Loveday, 2018). The mean value of this range (i.e., 30 kWh for a 100-mile drive) can be used in the estimation. The amount of coal needed to generate 30 kWh of electricity is around 10.71 lb, using the metric of 2.80 kWh per lb of coal (U.S. EIA, 2018). Literature shows that complete combustion of one pound of coal will lead to 2.86 lb CO_2 emission. Thus, the emission from driving 100 miles using an EV is around 30.63 lb. The actual emission may be higher than this number if the factors of incomplete combustion, low efficiency in power plant, and other processes required in electricity generation, transmission, and distribution are considered. Literature reports that the weighted average emission rate in the U.S. is 1.56 lb of CO_2 per kWh of electricity (U.S. EPA, 2018). When using this metric, the emission from driving 100 miles using an EV is around 45 lb.

For a traditional internal combustion engine vehicle using gasoline, the emission from driving 100 miles is estimated as follows. The fuel economy of new U.S. cars and trucks hit a record of 24.7 miles per gallon in the 2016 model year (Reuters, 2018), which indicates that around 4.1 gallons of gasoline are required for a 100-mile drive. The U.S. EIA also shows that the metric with respect to the emission per unit gallon of gasoline is 19.59 lb of CO_2 per gallon of gasoline (U.S. EPA, 2018). Thus, the emission for driving 100 miles using traditional internal combustion engine vehicles using gasoline is around 80.31 lb, which is much higher than the emissions of EVs.

In addition to such economic and environmental benefits from the perspective of the transportation sector, EV is also considered a critical supplementary resource for building a sustainable energy system under a smart grid environment. For example, the energy stored in the battery of EVs may have the potential for use as a backup energy source to the energy system in case failures happen to specific components of the energy system (Xia, Xi, Zhou, & Du, 2012).

Recently, the major economies around the world, such as the European Union and China, have announced their timetable to gradually phase out gas and diesel vehicles in the next two decades (Fox Business, 2017; Roberts, 2017). A number of automakers have started to accelerate new EV model introduction (Roberts, 2017). In addition to Tesla, traditional vehicle makers such as General Motors, Ford, and Toyota have also announced their plan to transform into EV-focused auto makers after 2020 (Holley, 2017).

A great number of studies have been implemented for various EV relevant topics, such as EV industry evolution (Liu, Huang, & Yang, 2017), EV charging station deployment (You & Hsieh, 2014), novel charging technology for EV (Ko, Jang, & Lee, 2015), etc. In particular, with an expectable growth trend toward an even higher market share in the near future, the impacts of EV usage on the existing electricity grid infrastructure, especially the additional load incurred by EV charging, have drawn wide research attention from both academia and industry. Various studies that focus on analyzing and quantifying such impacts have been reported (Clement-Nyns, Haesen, & Driesen, 2010; EPRI, 2007; Liu, Dow, & Liu, 2011; Richardson, 2013; Sovacool & Hirsh, 2009). The control strategies for optimal EV charging schedules have also been investigated (Ortega-Vazquez, Bouffard, & Silva, 2013; Rotering & Ilic, 2011; Sortomme & El-Sharkawi, 2011). For example, Ortega-Vazquez et al. (2013) proposed a necessary adaption scheme for the electricity market when the input of EV aggregation to the grid is considered. The common understanding is that a coordinated EV charging behavior will benefit the existing electricity infrastructure by accommodating additional demands, which is favorable to the entire electricity system during the charging period.

Meanwhile, the EVs' integration into the smart grid for improving grid reliability and service quality has been investigated (Dallinger, Krampe, & Wietschel, 2011; Guille & Gross, 2009; Liu, Chau, & Wu, 2013; Nezamoddini & Wang, 2017). For example, Dallinger et al. (2011) proposed a Vehicle-to-Grid (V2G) regulation reserve model based on a dynamic simulation of EVs' mobility behaviors. Nezamoddini and Wang (2017) proposed a stochastic model from the Independent System Operator's perspective for risk management and participation planning of EVs in the smart grid for different types of demand response programs. Moreover, the study on evaluating the benefits and risks of integrating the EVs into the smart grid has been explored (Ortega-Vazquez & Kintner-Meyer, 2015).

In general, the integration can be realized by three modes, including base load, peak load, and frequency regulation, as shown in Fig. 1. In base load mode, EVs are required to work as the regular generators to provide electricity to the grid. In peak load mode, EVs need to provide additional electricity supply during peak periods. In frequency regulation mode, EVs need to adjust the energy flow rate between the batteries and the grid to reduce the difference between the load and the generation of the grid so that the frequency of the grid can be tuned back from deviation on a real-time basis (Kempton & Tomic, 2005).

It has been pointed out that the cost due to the battery degradation is significant when EVs are used for base load and peak load purposes. In these two modes, each individual EV functions as an “energy storage device” for bulk energy service with a deeper depth of discharging and a longer service time (Kempton & Tomic, 2005). However, in the frequency regulation mode, the vehicle battery will undergo shallow charging/discharging cycles with a short duration, so the cost with respect to battery degradation is very limited compared to the application of an energy storage device used to provide bulk energy (Kempton, Udo, Huber, Komara, Letendre, Baker, & Pearre, 2008; Ortega-Vazquez & Kintner-Meyer, 2015). Furthermore, the frequency regulation mode requires that the sources providing regulation service possess a fast response capability (less than one minute) to either provide or consume the electricity in order to offset the unbalance between the generation and the load (Kempton & Tomic, 2005), which can be fulfilled by EVs. Therefore, the frequency regulation mode is considered a promising EV V2G application by many researchers (Brooks, 2002; Kempton, Tomic, Letendre, Brooks, & Lipman, 2001; Ortega-Vazquez & Kintner-Meyer, 2015).

In practice, when the EV is involved in frequency regulation and the grid frequency drops due to the fact that the load exceeds the generation, the signal of regulation up can be issued by the grid. The EVs can assist in “regulation up” by either decreasing the charging rate or increasing the discharging rate. On the other hand, if the frequency increases because the generation exceeds the load, the signal of regulation down can be issued by the grid. The EVs can assist in “regulation down” by either increasing the charging rate or decreasing the discharging rate. Note that, in some existing literature, regulation up and regulation down are achieved by discharging and charging, respectively, rather than the variation of the energy flow. This modeling strategy is largely based on the understanding that the energy flow between the EV and the grid is separated from the traditional or main load of the grid. In other words, compared to the traditional load of the grid, the EV integration is considered a small noise to the main load, and, thus, it can be used as a “third-party” separate source for the regulation. However, considering the fast growth of the EVs’ market, this part of load should be an integral part of the entire grid and cannot be considered independent of the regular load. Therefore, in this model, the energy variation compared to the previous period is considered (instead of the absolute energy flow of the current period) for measuring the actual contribution to the grid.

Furthermore, considering the limited size of an individual battery that can only provide 10–20 kW of power capacity (Kempton & Dhanju, 2006), multiple EVs need to be aggregated so that the total capacity is able to achieve the desired functionality in the frequency regulation mode. An intermediate aggregator between the grid and the EV owners is then needed to coordinate the aggregated EVs’ behaviors for frequency regulation when they are connected to the grid. The cost effectiveness of such an aggregated frequency regulation service has been analyzed. For example, Kempton and Tomic (2005) demonstrated that the frequency regulation is the most competitive EV application that can be utilized by the grid when the payment from the grid to the aggregator includes both a capacity reserved payment and an actual energy contribution payment. The Federal Energy Regulatory Commission (FERC) also issued Order 755-Frequency Regulation Compensation, requiring that the compensation of frequency regulation resources should include both a capacity payment and a performance payment for the energy quantity provided for the frequency regulation (Federal Energy Regulatory Commission, 2011).

Studies dedicated to the regulation service using aggregated EVs through the interaction between the aggregator and the EV owners have been reported. Many of them focused on the problems related to energy flow from grid to vehicle. For instance, Jin, Tang, and Ghosh (2013) studied an EV charging scheduling problem from a customer's perspective considering the static and dynamic charging scenarios. Zhang, Sun, Liu, Tan, Wang, and Tsang (2018) proposed an EV charging scheduling mechanism that controls the active and reactive charging power of EVs to provide joint voltage and frequency regulation in a distribution network. Falahati, Taher, and Shahidehpour (2016) proposed a smart charging method based on fuzzy controller where the charging process is performed with respect to the frequency deviation of grid and the state of charge of EV battery.

Besides considering a single energy flow direction, some efforts have also been made in developing models for implementing frequency regulation using EVs where both charging and discharging are considered. For example, Pahasa and Ngamroo (2015) proposed bidirectional charging/discharging and state of charge control of plug-in hybrid electric vehicles for a microgrid frequency stabilization using a multiple model predictive control. Shimizu, Masuta, Ota, and Yokoyama (2011) developed a load frequency control method in power systems using a V2G system based on the users’ convenience, considering both the charging and discharging capability of the EVs. Vahedipour-Dahraie, Rashidizaheh-Kermani, Najafi, Anvari-Moghaddam, and Guerrero (2017) proposed optimal charging/discharging scheduling for EVs with the goal of improving the frequency stability of a microgrid.

In addition to the energy flow direction, the objective in frequency regulation using aggregated EVs has also been investigated. Most of the articles in this area aim to maximize the profit of the aggregator or the EV owners. For example, Han, Han, and Sezaki (2010a,b) proposed an aggregator scheme that makes use of the distributed power of EVs to reserve grid scaled power for frequency regulation based on the predicted price of frequency regulation for selecting the time of charging and discharging for each individual EV. Later, Han, Han, and Sezaki (2011a) proposed an optimal control strategy for plug-in electric vehicles for V2G frequency regulation using quadratic programming. They also proposed a method of estimating the achievable power capacity for frequency regulation in a probabilistic manner to maximize the corresponding profit of the grid operator and EV aggregator (Han, Han, & Sezaki, 2011b).

However, most of the aforementioned research only considers the revenue due to the capacity reservation contributed by the EVs for potential charging/discharging while ignoring the benefits due to the actual energy contribution. Furthermore, when estimating the capacity reservation that can be contributed by the EVs in frequency regulation, the existing literature usually uses the maximum charging or discharging rates from the EVs being neither charged nor discharged. For example, Izadkhast, Garcia-Gonzalez, and Frías (2015) estimated the reserved capacity of aggregated EVs from the ones being neither charged nor discharged. Han et al. (2010a,b) employed the similar estimation philosophy to develop an optimal charging plan for frequency regulation using EVs. Likewise, Jian et al. (2015) developed a dynamic frequency response control strategy using EVs in the Great Britain power system where only the EVs being neither charged nor discharged are considered in reservation capability estimation. The possible contribution to the capacity reservation through varying the charging and discharging rates or switching the charging and discharging states has not been considered.

In addition, the concern of real-time problem solving based on the online system state and information has not been addressed yet. Most existing literature focused on solving an analytical optimization model for the entire planning horizon based on the prerequisite that all the conditions are known and deterministic in advance. The challenge to the EV aggregator when making decisions is that the control actions need to be dynamically updated together with the changing signals of the frequency regulation from the grid as well as the new EVs that are connected to the grid. The EV aggregator must address the problem considering not only the local (or current), but also the global (a long-time horizon including multiple request signals) optimality for the stability of the grid. The actual energy flow contribution needs to be determined considering not only the bonus payment, but also the tradeoff between "reservation for the future" and "utilization for now".

To address the aforementioned limitations and challenges, a dynamic decision-making model using the Markov Decision Process (MDP) is proposed in this paper for the EV aggregator to use in frequency regulation. The model utilizes online information such as real-time regulation signals, state of charge (SOC) of EVs, EV arrival (i.e., EVs that are newly connected to the grid) and departure (i.e., EVs that are disconnected from the grid), etc. The aggregator's revenue due to the reserved regulation capacity, the actual energy contributed (both charging and discharging), and the payment to the EV owners for the concern of battery degradation is modeled in the objective function. Moreover, the connected EVs at any state (charging, idle, and discharging) are considered as candidates that can contribute to the frequency regulation. The contribution for reserved capacity is computed based on their previous energy flow state rather than the idle state only. A semi-online solution strategy is proposed to find the near-optimal solution on a real-time basis. A numerical case study is used to illustrate the effectiveness of the proposed modeling strategy and solution approach. The remaining part of the paper is organized as follows. The proposed model formulation and real-time solution strategies are introduced in Section 2. A numerical case study is implemented in Section 3. The economic viability and the impacts on battery lifespan of the proposed method are discussed in Section 4. Finally, conclusions are drawn and future work is discussed in Section 5.

2. Proposed method

In this section, MDP is employed to establish a real-time decision making model for the aggregator of EVs to maximize its revenue in frequency regulation. The system state, control action, state transition, and objective function of the MDP model are introduced in Section 2.1. A semi-online solution strategy is then introduced to solve the formulated problem on a real-time basis in Section 2.2.

2.1. Model formulation

The decision horizon of the MDP model is discretized into a set of periods with constant duration of Δt. The frequency regulation signals issued by the utility companies are updated at the beginning of each period. Let t be the index of such periods. All the decisions are made at the beginning of period t. The EVs' connections to and disconnections from the grid are assumed to occur at the beginning of each period. In addition, it is assumed that there are two different charging rates, i.e., fast and regular charging rates, while a single discharging rate for each EV.

Let $\mathbf{DI}(t)$ be the set consisting of EVs that are dischargeable at period t. The EVs belong to this set satisfy the condition

$$\frac{C_i(SOC_i^{\mathrm{Re}q} - SOC_i^t)}{CHA_{h_i}\cdot\Delta t} < t_i^d - t \tag{1}$$

where C_i is the battery capacity of EV i. CHA_{h_i} is the fast charging rate of EV i. SOC_i^t is the state of charge (i.e., SOC, the ratio between the remaining capacity and the full capacity of the battery) of the battery of EV i at the beginning of period t. t_i^d is the index of the period of the estimated leaving time of EV i. SOC_i^{Req} is the required SOC of EV i at its estimated leaving time. The estimated leaving time and SOC_i^{Req} can be provided by each EV owner to the aggregator when the EV is connected to the grid. It is also assumed that all the EV owners are rational and thus, the estimated leaving time is obtained by the mean connection duration from their historical records. The reported SOC_i^{Req} will not beyond the maximally achievable SOC based on the fast charging rate as well as the estimated connection duration of EV i.

Eq. (1) describes that the discharging can be considered when the time duration between the current period t and the EV's estimated leaving time is long enough so that the EV can be charged to SOC_i^{Req}, using fast charging rate. It can be rewritten as

$$SOC_i^t\cdot C_i > SOC_i^{\mathrm{Re}q}\cdot C_i - CHA_{h_i}\cdot(t_i^d - t)\cdot\Delta t \tag{2}$$

Let CHA_{l_i} be the regular charging rate of EV i. Let $\mathbf{CH_H}(t)$ be the set including the EVs that are chargeable with fast charging rate at time t. Let $\mathbf{CH_{L\cap\bar{H}}}(t)$ be the set consisting of the EVs that are chargeable with regular charging rate, but non-chargeable with fast charging rate at time t. The EVs belong to $\mathbf{CH_H}(t)$ and $\mathbf{CH_{L\cap\bar{H}}}(t)$ meet the conditions (3) and (4) below, respectively.

$$SOC_i^t\cdot C_i \leqslant C_i - CHA_{h_i}\cdot\Delta t \tag{3}$$

$$C_i - CHA_{h_i}\cdot\Delta t < SOC_i^t\cdot C_i \leqslant C_i - CHA_{l_i}\cdot\Delta t \tag{4}$$

Based on the sets defined above, all the EVs can be categorized into six different groups at time t as shown in Table 1.

For the EVs belong to group 1, they satisfy the condition (5).

$$SOC_i^{\mathrm{Re}q}\cdot C_i - CHA_{h_i}\cdot(t_i^d - t)\cdot\Delta t < SOC_i^t\cdot C_i \leqslant C_i - CHA_{h_i}\cdot\Delta t \tag{5}$$

For the EVs belong to group 2, they satisfy the condition (6).

$$\max(C_i - CHA_{h_i}\cdot\Delta t,\ SOC_i^{\mathrm{Re}q}\cdot C_i - CHA_{h_i}\cdot(t_i^d - t)\cdot\Delta t) < SOC_i^t\cdot C_i \leqslant C_i - CHA_{l_i}\cdot\Delta t \tag{6}$$

For the EVs belong to group 3, they satisfy the condition (7).

$$SOC_i^t\cdot C_i < \min(SOC_i^{\mathrm{Re}q}\cdot C_i - CHA_{h_i}\cdot(t_i^d - t)\cdot\Delta t,\ C_i - CHA_{h_i}\cdot\Delta t) \tag{7}$$

For the EVs belong to group 4, they satisfy the condition (8).

$$C_i - CHA_{h_i}\cdot\Delta t < SOC_i^t\cdot C_i < \min(SOC_i^{\mathrm{Re}q}\cdot C_i - CHA_{h_i}\cdot(t_i^d - t)\cdot\Delta t,\ C_i - CHA_{l_i}\cdot\Delta t) \tag{8}$$

For the EVs belong to group 5, they satisfy the condition (9).

$$SOC_i^t\cdot C_i > \max(SOC_i^{\mathrm{Re}q}\cdot C_i - CHA_{h_i}\cdot(t_i^d - t)\cdot\Delta t,\ C_i - CHA_{l_i}\cdot\Delta t) \tag{9}$$

For the EVs belong to group 6, they satisfy the condition (10).

$$C_i - CHA_{l_i}\cdot\Delta t < SOC_i^t\cdot C_i < SOC_i^{\mathrm{Re}q}\cdot C_i - CHA_{h_i}\cdot(t_i^d - t)\cdot\Delta t \tag{10}$$

System state. The system state at decision period t is defined as the capacities reserved by the aggregator for regulation up (RES_{up}^t) and regulation down (RES_{dn}^t). RES_{up}^t and RES_{dn}^t can be formulated by

$$RES_{up}^t = \sum_i \Delta p_i^{t+}\cdot\Delta t \tag{11}$$

Table 1
Six groups of EVs.

#	Descriptions
1	Chargeable with fast charging rate and dischargeable
2	Chargeable only with regular charging rate and dischargeable
3	Chargeable with fast charging rate and not dischargeable
4	Chargeable only with regular charging rate and not dischargeable
5	Dischargeable and not chargeable
6	Neither chargeable nor dischargeable

$$RES_{dn}^{t} = \sum_{i} \Delta p_i^{t-} \cdot \Delta t \tag{12}$$

where Δp_i^{t+} and Δp_i^{t-} are the maximum achievable contributions from EV i to the reserved capacities of regulation up and regulation down, respectively at period t. On one hand, if considering the energy flow from the EV to the grid, they can be the maximally achievable increase and reduction of energy flow, respectively, at period t compared to period $t-1$. On the other hand, if considering the energy flow from the grid to the EV, they can be the maximally achievable reduction and increase of energy flow, respectively, at period t compared to period $t-1$.

For the EVs belong to group 1, Δp_i^{t+} and Δp_i^{t-} can be formulated as

$$\Delta p_i^{t+} = A_i^{t-1} - DIS_i \tag{13}$$

$$\Delta p_i^{t-} = CHA_{h_i} - A_i^{t-1} \tag{14}$$

where DIS_i is the discharging rate of EV i. For convenience, the charging rate is represented by positive number, while a negative number represents the discharging rate of EV i. A_i^{t-1} in Eqs. (13) and (14) is the energy flow rate of EV i in period $t-1$. It can be equal to either CHA_{h_i}, CHA_{l_i}, DIS_i, or zero, depending on the actions adopted by EV i in period $t-1$ (zero is used for the action of leave alone).

For the EVs belong to group 2, Δp_i^{t+} and Δp_i^{t-} can be calculated by

$$\Delta p_i^{t+} = A_i^{t-1} - DIS_i \tag{15}$$

$$\Delta p_i^{t-} = \max(CHA_{l_i} - A_i^{t-1}, 0) \tag{16}$$

For the EVs belong to group 3, Δp_i^{t+} and Δp_i^{t-} can be calculated by

$$\Delta p_i^{t+} = \max(A_i^{t-1}, 0) \tag{17}$$

$$\Delta p_i^{t-} = CHA_{h_i} - A_i^{t-1} \tag{18}$$

For the EVs belong to group 4, Δp_i^{t+} and Δp_i^{t-} can be calculated by

$$\Delta p_i^{t+} = \max(A_i^{t-1}, 0) \tag{19}$$

$$\Delta p_i^{t-} = \max(CHA_{l_i} - A_i^{t-1}, 0) \tag{20}$$

For the EVs belong to group 5, Δp_i^{t+} and Δp_i^{t-} can be calculated by

$$\Delta p_i^{t+} = A_i^{t-1} - DIS_i \tag{21}$$

$$\Delta p_i^{t-} = \max(-A_i^{t-1}, 0) \tag{22}$$

For the EVs belong to group 6, Δp_i^{t+} and Δp_i^{t-} can be calculated by

$$\Delta p_i^{t+} = \max(A_i^{t-1}, 0) \tag{23}$$

$$\Delta p_i^{t-} = \max(-A_i^{t-1}, 0) \tag{24}$$

Note that for the EVs that are newly connected to the grid at period t, A_i^{t-1} can be set as zero.

Control action. The aggregator needs to determine the actions, i.e., either fast charging, or regular charging, or discharging, or leave alone for each individual EV at the beginning of period t. Let $\mathbf{A}_t$ be the actions adopted by the aggregator for all the EVs at the beginning of period t. Considering the potential computational challenge due to the huge amount of state-action pairs, an action aggregation strategy is adopted in this research by assigning all the EVs to the six groups (Islam, Sun, & Qin, 2018) defined in Table 1. The aggregator will determine the optimal actions for each group so that the number of the state-action pairs can be effectively reduced. The details of the feasible control actions for each group are given in Table 2.

State transition. As mentioned, the EV owners' estimations of their respective durations when the EVs are connected to the grid are close to the actual connection durations. The uncertainty of the actual connection time can be modeled as a random variable following a certain distribution. Such a distribution can be approximated from the historical records of EV motion pattern, which is assumed to be known by both EV owner and aggregator. The estimated and reported connection duration can be the mean of such a random variable. Let K_i be the random variable of the actual connection duration of EV i. Let $T(t)$ be the connection duration up to the beginning of period t. Let g_i^{t+1} denote the probability that EV i will be disconnected from the grid at the period $t+1$. g_i^{t+1} can be calculated by

$$g_i^{t+1} = \Pr(K_i \leqslant T(t+1)|\ K_i > T(t)) = \frac{F_i(T(t+1)) - F_i(T(t))}{1 - F_i(T(t))} \tag{25}$$

where $F_i(T(t))$ is the cumulative distribution function of the random variable of actual connection duration of EV i. It is assumed that K_i follows the exponential distribution with mean of u_i. $F_i(T(t))$ can be calculated by

$$F_i(T(t)) = 1 - e^{-T(t)/u_i} \tag{26}$$

Let N_t be the total number of EVs that are connected to the grid at the beginning of period t. For a certain amount of EVs, say h, that will be disconnected from the grid at period $t+1$, there exist $\binom{N_t}{h}$ different combinations to form such an h-EV group out of total N_t EVs. Let n_h be the index of such combinations. Let Ω_{n_h} be the set consisting of h disconnected EVs according to combination n_h. It is assumed that the disconnections from the grid of various EVs are mutually independent. Let $L^{t+1}(n_h)$ be the probability that certain group of h EVs according to combination n_h are disconnected from the grid at time $t+1$. $L^{t+1}(n_h)$ can be calculated by

$$L^{t+1}(n_h) = \begin{cases} \prod_{i \in \Omega_{n_h}} g_i^{t+1}, & h > 0 \\ \prod_{i=1}^{N_t} (1 - g_i^{t+1}), & h = 0 \end{cases} \tag{27}$$

Also it is assumed that the number of EVs that will be connected to the grid at period $t+1$ follows Poisson distribution with mean of λ_{t+1}. Let $I^{t+1}(q)$ be the probability that q EVs are connected to the grid at period $t+1$, which can be formulated by

$$I^{t+1}(q) = \frac{\lambda_{t+1}^{q} e^{-\lambda_{t+1}}}{q!} \tag{28}$$

Let Q_{t+1} be the minimum value so that the cumulative distribution function of the Poisson distribution, $F(Q_{t+1})$, is larger than or equal to a given threshold value, say, 99%. Q_{t+1} is used to approximate the maximum number of newly connected EVs at period $t+1$.

The expected value of the reserved capacity of regulation up at period $t+1$ can be calculated by

$$RES_{up}^{t+1} = RES_{up}^{t+1}(\mathbf{S}_t,\ \mathbf{A}_t) - \Delta RES_{L-up}^{t+1} + \Delta RES_{A-up}^{t+1} \tag{29}$$

where $RES_{up}^{t+1}(\mathbf{S}_t,\ \mathbf{A}_t)$ is the reserved capacity of regulation up at period $t+1$ due to the action $\mathbf{A}_t$ adopted at given state $\mathbf{S}_t$ at period t. ΔRES_{L-up}^{t+1} is the expected decrease of the reserved capacity of regulation up due to the EVs' disconnections from the grid at period $t+1$. ΔRES_{A-up}^{t+1} is the expected increase of the reserved capacity of regulation up due to the EVs that are newly connected to the grid at period $t+1$. $RES_{up}^{t+1}(\mathbf{S}_t,\ \mathbf{A}_t)$ can be calculated by

$$RES_{up}^{t+1}(\mathbf{S}_t,\ \mathbf{A}_t) = \sum_{i} \Delta p_i^{(t+1)+} \cdot \Delta t \tag{30}$$

To calculate $\Delta p_i^{(t+1)+}$ in Eq. (30), it is required to select the equation from Eqs. (13), (15), (17), (19), (21), and (23) depending on the group that EV i belongs to at period $t+1$. To map each EV into the appropriate group, the SOC of the EV i at period $t+1$ needs to be updated using

$$SOC_i^{t+1} = (SOC_i^{t} \cdot C_i + Cha_{ih}^{t} \cdot \Delta t + Dis_i^{t} \cdot \Delta t + Cha_{il}^{t} \cdot \Delta t + La_i^{t} \cdot \Delta t)/C_i \tag{31}$$

where Cha_{ih}^{t} is the energy flow rate when the action of fast charging is selected for EV i at period t. Cha_{il}^{t} is the energy flow rate when the action of regular charging is selected for EV i at period t. Dis_i^{t} is the

Table 2
Possible actions for the EVs in each group.

#	Descriptions	Feasible Actions
1	Chargeable with fast charging rate and dischargeable	Charging with either fast or regular charging rates, discharging, or leave alone
2	Chargeable only with regular charging rate and dischargeable	Charging with regular charging rate, discharging, or leave alone
3	Chargeable with fast charging rate and not dischargeable	Charging with either fast or regular charging rates, or leave alone
4	Chargeable only with regular charging rate and not dischargeable	Charging with regular charging rate, or leave alone
5	Dischargeable and not chargeable	Discharging, or leave alone
6	Neither chargeable nor dischargeable	Leave alone

energy flow rate when the action of discharging is selected for EV i at period t. La_i^t is the energy flow rate when the action of leave alone is selected for EV i at period t. Recall that positive number, negative number, and zero are used to denote the energy flow rates due to charging, discharging, and leave alone, respectively.

Also, ΔRES_{L-up}^{t+1} can be calculated by

$$\Delta RES_{L-up}^{t+1} = \begin{cases} \sum_{h=1}^{N^t} \sum_{n_h=1}^{\binom{N^t}{h}} L^{t+1}(n_h)\cdot \sum_{i\in\Omega_{n_h}} \Delta p_i^{(t+1)+}\cdot\Delta t,\ h>0 \\ 0,\ h=0 \end{cases} \tag{32}$$

ΔRES_{A-up}^{t+1} can be calculated by

$$\Delta RES_{A-up}^{t+1} = \begin{cases} \sum_{q=1}^{Q_{t+1}} I^{t+1}(q)\cdot \sum_{k_q} \Delta p_{k_q}^{(t+1)+}\cdot\Delta t,\ \ q>0 \\ 0,\ \ q=0 \end{cases} \tag{33}$$

where k_q is the index of the q EVs that are connected to the grid at period $t+1$, $k_q = 1, \ldots, q$. $\Delta p_{k_q}^{(t+1)+}$ can be calculated following the similar procedure aforementioned (The action of leave alone is considered the $A_{k_q}^{t-1}$ for EV k_q).

Similarly, the expected value of the reserved capacity of regulation down at period $t+1$ can be calculated by

$$RES_{dn}^{t+1} = RES_{dn}^{t+1}(\mathbf{S}_t,\ \mathbf{A}_t) - \Delta RES_{L-dn}^{t+1} + \Delta RES_{A-dn}^{t+1} \tag{34}$$

where $RES_{dn}^{t+1}(\mathbf{S}_t,\ \mathbf{A}_t)$ is the reserved capacity of regulation down at period $t+1$ due to the action $\mathbf{A}_t$ adopted at given state $\mathbf{S}_t$ at period t. ΔRES_{L-dn}^{t+1} is the expected decrease of the reserved capacity of regulation down due to the EVs' disconnections from the grid at period $t+1$. ΔRES_{A-dn}^{t+1} is the expected increase of the reserved capacity of regulation down due to the EVs that are newly connected to the grid at period $t+1$. $RES_{dn}^{t+1}(\mathbf{S}_t,\ \mathbf{A}_t)$ can be formulated as

$$RES_{dn}^{t+1}(\mathbf{S}_t,\ \mathbf{A}_t) = \sum_i \Delta p_i^{(t+1)-}\cdot\Delta t \tag{35}$$

where $\Delta p_i^{(t+1)-}$ can be calculated by selecting the equation from Eqs. (14), (16), (18), (20), (22), and (24) depending on the group that EV i belongs to at period $t+1$. Also, ΔRES_{L-dn}^{t+1} can be calculated by

$$\Delta RES_{L-dn}^{t+1} = \begin{cases} \sum_{h=1}^{N^t} \sum_{n_h=1}^{\binom{N^t}{h}} L^{t+1}(n_h)\cdot \sum_{i\in\Omega_{n_h}} \Delta p_i^{(t+1)-}\cdot\Delta t,\ \ h>0 \\ 0,\ \ h=0 \end{cases} \tag{36}$$

and ΔRES_{A-dn}^{t+1} can be calculated by

$$\Delta RES_{A-dn}^{t+1} = \begin{cases} \sum_{q=1}^{Q_{t+1}} I^{t+1}(q)\cdot \sum_{k_q} \Delta p_{k_q}^{(t+1)-}\cdot\Delta t,\ \ q>0 \\ 0,\ \ q=0 \end{cases} \tag{37}$$

where $\Delta p_{k_q}^{(t+1)-}$ can be calculated following the similar procedure (Again, the action of leave alone is considered the $A_{k_q}^{t-1}$ for EV k_q). A graphical illustration of the state transition is shown in Fig. 2.

Objective function. The function of the revenue that can be obtained by the aggregator from current decision period t to the end of planning horizon incurred by adopting action $\mathbf{A}_t$ at given state $\mathbf{S}_t$ can be formulated by

$$R(\mathbf{S}_t,\ \mathbf{A}_t) + \sum_{\mathbf{S}'} Pr(\mathbf{S}_{t+1} = \mathbf{S}'|\ \mathbf{S}_t,\ \mathbf{A}_t)\cdot V(\mathbf{S}_{t+1}) \tag{38}$$

where $R(\mathbf{S}_t,\ \mathbf{A}_t)$ is the immediate revenue incurred in period t due to the adopted action $\mathbf{A}_t$ based on given state $\mathbf{S}_t$. $Pr(\mathbf{S}' = \mathbf{S}_{t+1}|\ \mathbf{S}_t,\ \mathbf{A}_t)$ is the transition probability that the state at period $t+1$ is $\mathbf{S}'$ given $\mathbf{S}_t$ and $\mathbf{A}_t$. $V(\mathbf{S}_{t+1})$ is the subsequent revenue from period $t+1$ to the end of the decision making horizon given the state at period $t+1$.

In frequency regulation, the revenue originates from both capacity reserved and actual energy contributed. Also, considering the payment to the EV owners for the possible battery degradation due to discharging and fast charging in frequency regulation, $R(\mathbf{S}_t,\ \mathbf{A}_t)$ can be calculated by

$$R(\mathbf{S}_t,\ \mathbf{A}_t) = B(\mathbf{S}_t,\ \mathbf{A}_t) + P(\mathbf{S}_t,\ \mathbf{A}_t) - D(\mathbf{S}_t,\ \mathbf{A}_t) - F(\mathbf{S}_t,\ \mathbf{A}_t) \tag{39}$$

where $B(\mathbf{S}_t,\ \mathbf{A}_t)$ is the revenue obtained due to the actual energy flow variation contributed at period t for providing service of frequency regulation. $P(\mathbf{S}_t,\ \mathbf{A}_t)$ is the revenue due to the capacity reserved for both regulation up and regulation down at period t. $D(\mathbf{S}_t,\ \mathbf{A}_t)$ is the cost considering battery degradation when discharging at period t. $F(\mathbf{S}_t,\ \mathbf{A}_t)$ is considered the battery degradation cost at period t when the fast charging is adopted.

It is assumed that for charging activities, the grid will charge the aggregator based on the given rate ($/kWh) disregarding the fact whether such a charging activity can vary the energy flow between the grid and the EVs (compared to the last period) to accommodate the desired direction specified by regulation signals issued by grid or not. If the energy flow variation can match desired direction, bonus will be counted additionally. Also, it is assumed that the price of the electricity purchased from the grid by the aggregator for EV charging is equal to the price paid by the EV owners to the aggregator. In other words, the aggregator will not make profit over the EV owners by providing charging service. Therefore, the terms of aggregator's cost to purchase electricity from grid to provide charging service for EVs and the aggregator's income from the EV owners for charging are canceled.

When regulation up is required, i.e., the decreasing charging energy or the increasing discharging energy compared to the last period is preferred, $B(\mathbf{S}_t,\ \mathbf{A}_t)$ can be formulated as

$$\begin{aligned} B(\mathbf{S}_t,\ \mathbf{A}_t) = b_{aup}^t\cdot[\max(0,\ (&\textstyle\sum_{i\in\mathbf{CHA}_l^{t-1}} Cha_{il}^{t-1} + \sum_{i\in\mathbf{CHA}_h^{t-1}} Cha_{ih}^{t-1} \\ &+ \textstyle\sum_{i\in\mathbf{DIS}^{t-1}} Dis_i^{t-1}) \\ &-(\textstyle\sum_{i\in\mathbf{CHA}_l^t} Cha_{il}^t + \sum_{i\in\mathbf{CHA}_h^t} Cha_{ih}^t + \sum_{i\in\mathbf{DIS}^t} Dis_i^t)]\cdot \\ &\Delta t \end{aligned} \tag{40}$$

where b_{aup}^t is the bonus rate for actual variation of energy flow towards the desired direction of regulation up at period t. $\mathbf{DIS}^t$ is the set of EVs that are discharged at period t. $\mathbf{CHA}_l^t$ and $\mathbf{CHA}_h^t$ are the sets of EVs that are charged with regular charging rate and fast charging rate, respectively, at period t.

Similarly, when regulation down is required, i.e., the increasing charging energy or the decreasing discharging energy compared to the last period is preferred, $B(\mathbf{S}_t,\ \mathbf{A}_t)$ can be formulated as

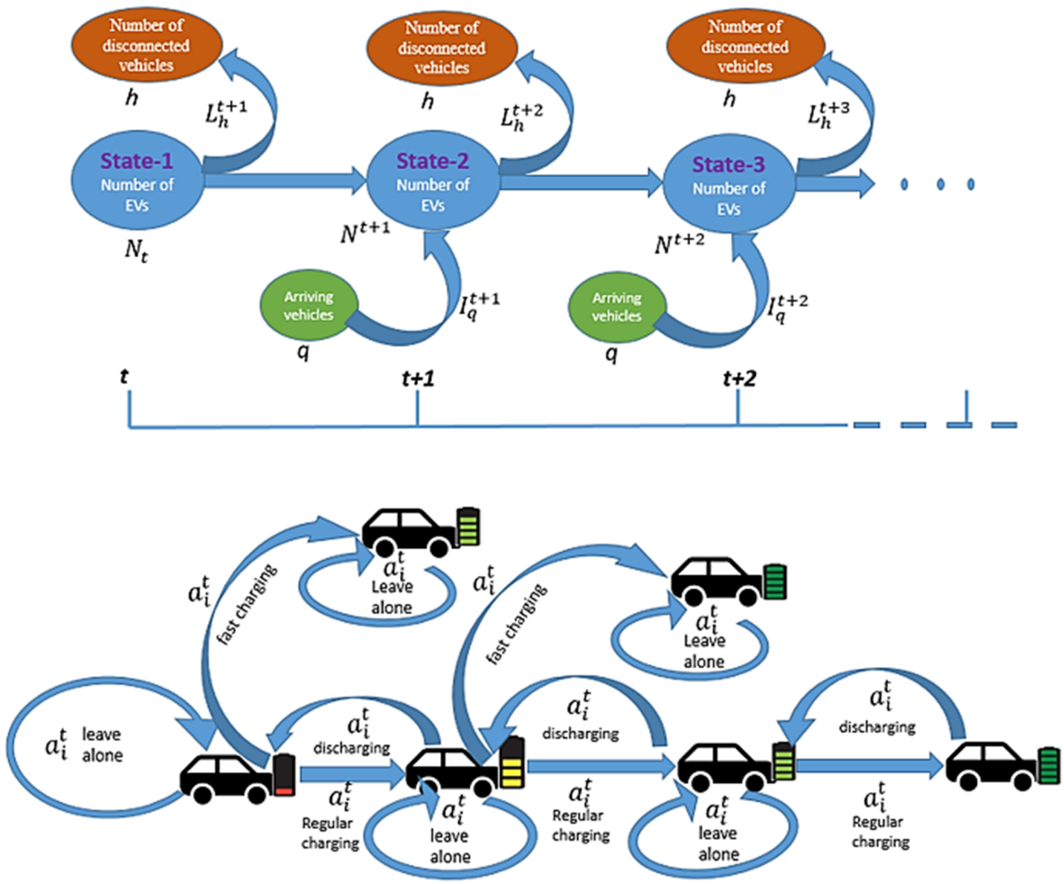

Fig. 2. State transition diagram in MDP model.

$$B(\mathbf{S}_t,\ \mathbf{A}_t) = b_{adn}^t \cdot [\max(0,\ (\textstyle\sum_{i\in \mathbf{CHA}_l^t} Cha_{il}^t + \sum_{i\in \mathbf{CHA}_h^t} Cha_{ih}^t + \sum_{i\in \mathbf{DIS}^t} Dis_i^t) - (\sum_{i\in \mathbf{CHA}_l^{t-1}} Cha_{il}^{t-1} + \sum_{i\in \mathbf{CHA}_h^{t-1}} Cha_{ih}^{t-1} + \sum_{i\in \mathbf{DIS}^{t-1}} Dis_i^{t-1})] \cdot \Delta t \tag{41}$$

where b_{adn}^t is the bonus rate for actual variation of energy flow towards the desired direction of regulation down.

$P(\mathbf{S}_t,\ \mathbf{A}_t)$ can be formulated by

$$P(\mathbf{S}_t,\ \mathbf{A}_t) = b_{rup}^t \cdot (RES_{up}^t + RES_{up}^{t+1})/2 + b_{rdn}^t \cdot (RES_{dn}^t + RES_{dn}^{t+1})/2 \tag{42}$$

where b_{rup}^t *and* b_{rdn}^t are the rates of the bonus that the aggregator can receive for unit capacity reserved for regulation up and regulation down, respectively, at period t. Since the capacity reserved for either up or down is not necessarily constant throughout the duration of a certain period t depending on the adopted actions $\mathbf{A}_t$, an average value is used to represent the capacity reserved in the period t in Eq. (42) for calculation.

$D(\mathbf{S}_t,\ \mathbf{A}_t)$ and $F(\mathbf{S}_t,\ \mathbf{A}_t)$ can be formulated as

$$D(\mathbf{S}_t,\ \mathbf{A}_t) = d \cdot \sum_{i\in \mathbf{DIS}^t} Dis_i^t \cdot \Delta t \tag{43}$$

$$F(\mathbf{S}_t,\ \mathbf{A}_t) = f \cdot \sum_{i\in \mathbf{CHA}_h^t} Cha_{ih}^t \cdot \Delta t \tag{44}$$

where d and f are the rates that the aggregator will pay to the EV owners for discharging and fast charging unit energy, respectively, in frequency regulation (\$/kWh). Thus, the objective function can be formulated as

$$\max_{\mathbf{A}_t} \left[R(\mathbf{S}_t,\ \mathbf{A}_t) + \sum_{\mathbf{S}'} Pr(\mathbf{S}_{t+1} = \mathbf{S}' |\ \mathbf{S}_t,\ \mathbf{A}_t) \cdot V(\mathbf{S}_{t+1})\right] \tag{45}$$

2.2. Solution technique

In Section 2.1, the decision making model of frequency regulation using aggregated EVs has been established under the framework of MDP. The classical tool to solve MDP is dynamic programming which begins its algorithm at the final decision period and steps back by looping over all the possible states and available actions until the optimal action for the current period is obtained (Bellman, 1957). Zero can be set as the estimation of the value function to denote the subsequent revenue for all the states at the final decision period.

However, the usefulness of backward method is limited due to the “curse of dimensionality” (Huang & Ma, 2011), which requires the algorithm to loop over all the states and actions, leading to computational intractability. Thus, an alternative of using a forward based approximate algorithm has been proposed (Powell, 2007). The basic idea of this forward algorithm is to begin the algorithm at the current time, and initialize a set of estimated values for value functions of all states for each decision period. A set of sample paths is randomly generated to simulate the evolution of system state. The algorithm runs from the current decision period to the final period along each sample path iteratively. The optimal decisions at each time period in each iteration can be identified by comparing the sum of the immediate revenue that can be explicitly calculated based on adopted actions $\mathbf{A}_t$ at given state $\mathbf{S}_t$ as well as the subsequent revenue based on the estimated value function. The value function is updated accordingly with each step and will be used for the next iteration and the corresponding optimal decisions can also be updated. The algorithm can be terminated when a predetermined number of iterations is reached or the error can be ensured to be bounded within a predetermined range.

Many algorithms such as reinforcement learning, Monte-Carlo based methodology, Q-learning, etc., based on such a forward based approximation have been proposed (Powell, 2007). The advantage of forward method over the backward one is that it avoids the calculation of looping over all possible states (Powell, 2007). However, it still requires the calculation of the expectation of value function in the next decision period, which is often computationally intractable if the size of reachable states at the next decision period is too large (Du, Xu, Huang, & Yao, 2015; Powell, 2007).

In addition, the time resolution of the proposed frequency regulation model can be quite high. Typically, every several minutes, the frequency regulation signal may be updated and thus the new decision needs to be identified on a real-time basis. Therefore, the problem formulated can involve around hundreds of decision periods if the planning horizon can be around ten hours and so the time to complete the simulation following an individual sample path will not be short. Furthermore, the estimation of the value function at decision period t through the final period is not easy and so zero is often used as approximation when initiating. Unlike the backward method whose value function is estimated from the final decision period and thus zero is a reasonable initial value, huge error exists between initial estimation and actual value, thus a great number of iterations running from the current period to the final period are required to smooth the error by updating the estimated value per each iteration (Powell, 2007), therefore it is very hard to obtain an approximate optimal solution in real-time.

In this research, a semi-online real-time solver is proposed to solve this problem on a real-time basis. The near optimal solution will be identified by comparing the sum of the immediate revenue $R(\mathbf{S}_t,\ \mathbf{A}_t)$ incurred in period t due to the adopted action $\mathbf{A}_t$ at given state $\mathbf{S}_t$ and the estimation of the expected value of the subsequent revenue from period $t+1$ to the end of the planning horizon, $\sum_{\mathbf{S}'} Pr(\mathbf{S}_{t+1}=\mathbf{S}'|\ \mathbf{S}_t,\ \mathbf{A}_t)\cdot V(\mathbf{S}_{t+1})$. The former can be calculated online on a real-time basis. The latter will be obtained from a lookup table that is built through offline simulation.

Offline simulation model. At first, a heuristic control strategy is considered based on a set of predetermined rules as the baseline scenario to run the offline simulation to find the value functions with different states at different periods. In the baseline scenario, the EVs' connections to and disconnections from the grid at each period are simulated following the given distributions. At period t when regulation up is required, discharging will be considered the action of the EVs in groups one, two, and five if the SOC of EV is higher than 50% and discharging decision was not adopted by the EV at period $t-1$. Otherwise, the actions that can lower the energy flow from the grid to the EVs (e.g., switch the EVs from fast charging to regular charging, from regular charging to leave alone) will be randomly selected for the EVs considering the feasibility of the actions in different groups. For regulation down, the action that can lead to an increasing energy flow from the grid to the EVs or a decreasing energy flow from the EVs to the grid compared to period $t-1$ (e.g., switch the EVs from leave alone to regular charging, from regular charging to fast charging, and from discharging to leave alone) will be randomly selected for the EVs considering the feasibility of the actions in different groups.

After running the offline simulation model using such a heuristic control strategy with multiple replications, the value functions for various states at different periods when the heuristic strategy is adopted ($V_h(\mathbf{S}_t)$) can be obtained and recorded as benchmark estimations.

Lookup table. A myopic one-step ahead approximation method is implemented to solve the problem. That is, at each period t, the optimal actions are obtained by minimizing the immediate revenue $R(\mathbf{S}_t,\ \mathbf{A}_t)$ (see next section for the calculation of $R(\mathbf{S}_t,\ \mathbf{A}_t)$). Such an approximation idea by looking one-step ahead in solving MDP problem has been used and obtained appealing results (Li & Sun, 2013). Thus, the ratio (γ_t) between the immediate revenue obtained by the actions adopted following the one-step ahead optimization strategy and the revenue obtained using the heuristic strategy in baseline simulation is used to approximately reflect the improvement potential of the value function at various periods under different states due to the adoption of the proposed model compared to the heuristic strategy. The ratio (γ_t) will be multiplied to the identified benchmark estimation ($V_h(\mathbf{S}_t)$) to obtain the approximated value functions from period t to the end when the proposed model is adopted ($\gamma_t\cdot V_h(\mathbf{S}_t)$). These approximated value functions for all states and periods are used to build the lookup table from which the estimation of the subsequent revenue can be identified by given states when the proposed solution algorithm is triggered.

Approximate immediate revenue. $R(\mathbf{S}_t,\ \mathbf{A}_t)$ can be explicitly calculated based on the adopted actions $\mathbf{A}_t$ at given state $\mathbf{S}_t$. The challenge to find the immediate revenue on a real-time basis is due to the use of Eqs. (29) and (34) in finding the reserved capacity of regulation up and regulation down at period $t+1$, respectively for calculating $P(\mathbf{S}_t,\ \mathbf{A}_t)$ in Eq. (42). The calculations of ΔRES_{L-up}^{t+1} and ΔRES_{L-dn}^{t+1} using Eqs. (32) and (36) need to loop over all the possible combinations of different numbers of the EVs that will be disconnected from the grid out of entire EV group, which may not be completed on a real-time basis. Thus, Eqs. (46) and (47) are proposed as the alternatives to estimate the expected value of the reserved capacities of regulation up and regulation down at period $t+1$, respectively, for the calculation of $P(\mathbf{S}_t,\ \mathbf{A}_t)$ in (42).

$$RES_{up}^{t+1}=\sum_i (1-g_i^{t+1})\cdot\Delta p_i^{(t+1)+}\cdot\Delta t+\Delta RES_{A-up}^{t+1} \tag{46}$$

$$RES_{dn}^{t+1}=\sum_i (1-g_i^{t+1})\cdot\Delta p_i^{(t+1)-}\cdot\Delta t+\Delta RES_{A-dn}^{t+1} \tag{47}$$

The first terms on the right-hand sides of Eqs. (46) and (47) are the expected values of the reserved capacities of regulation up and down, respectively, at period $t+1$ contributed by the EVs that are connected to the grid at period t. They are used to circumvent the calculation when looping over all the possible combinations of various numbers of disconnection EVs in Eqs. (32) and (36).

Approximate subsequent revenue. When calculating the term $\sum_{\mathbf{S}'} Pr(\mathbf{S}_{t+1}=\mathbf{S}'|\ \mathbf{S}_t,\ \mathbf{A}_t)\cdot V(\mathbf{S}_{t+1})$, it is required to identify each reachable state $\mathbf{S}_{t+1}$ at period $t+1$ so that the value function $V(\mathbf{S}_{t+1})$ can be obtained from the lookup table as well as the corresponding transition probability $Pr(\mathbf{S}_{t+1}=\mathbf{S}'|\ \mathbf{S}_t,\ \mathbf{A}_t)$. Considering various possibilities of connection and disconnection EVs at period $t+1$, it is hard to loop over all the reachable states on a real-time basis to calculate the expected value. Therefore, Eqs. (48) and (49) are proposed as the alternatives to estimate the possible states at period $t+1$ considering the new connections of q EVs at period $t+1$.

$$RES(q)_{up}^{t+1}=\sum_i (1-g_i^{t+1})\cdot\Delta p_i^{(t+1)+}\cdot\Delta t+I^{t+1}(q)\cdot\Delta p^{(t+1)+}(q)\cdot\Delta t \tag{48}$$

$$RES(q)_{dn}^{t+1}=\sum_i (1-g_i^{t+1})\cdot\Delta p_i^{(t+1)-}\cdot\Delta t+I^{t+1}(q)\cdot\Delta p^{(t+1)-}(q)\cdot\Delta t \tag{49}$$

where $RES(q)_{up}^{t+1}$ and $RES(q)_{dn}^{t+1}$ are the reserved capacities for regulation up and regulation down, respectively, at period $t+1$ due to the new connections of q EVs. $\Delta p^{(t+1)+}(q)$ and $\Delta p^{(t+1)-}(q)$ are the maximally achievable contributions to the reserved capacities of regulation up and regulation down, respectively, from the q EVs that are connected to the grid at period $t+1$. In the offline simulation model, at each period, the contributions to reserved capacities of regulation up and regulation down due to the newly connected EVs are recorded. $\Delta p^{(t+1)+}(q)$ and $\Delta p^{(t+1)-}(q)$ are identified using the mean of the recorded contributions when q EVs are newly connected at period $t+1$. Using Eqs. (48) and (49), the number of reachable system states at period $t+1$ is reduced to $Q_{t+1}+1$ by smoothing the different contributions to the reserved capacity led by various EV brands, SOC states, battery capacities, etc., through an average value from offline simulations.

To further reduce the dimension of the reachable states at period $t+1$, it is also proposed to use the aggregation strategy to aggregate all possible different reachable states into a few groups. The size of the

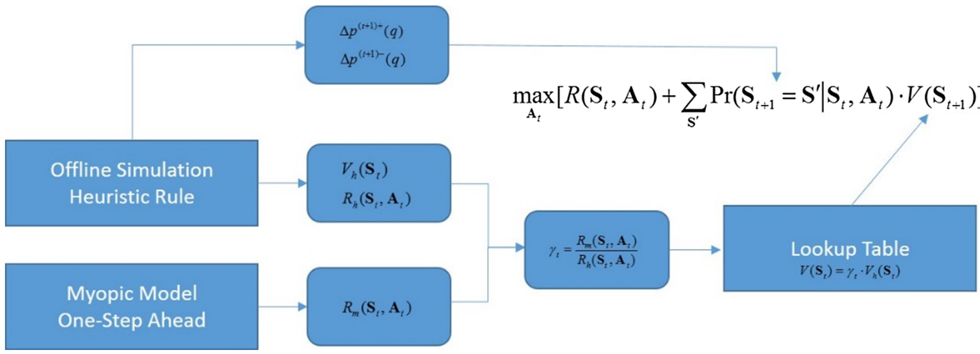

Fig. 3. Real-time solution strategy.

group is predetermined so that various q values fall in the range specified by the size will be considered in the same group. The transition probability to such an aggregated state is approximately calculated by averaging the probabilities of all the numbers of new connection EVs at period t included in the predetermined range. The contribution to the reserved capacity is also estimated through such an average approximation.

The overall procedure of the solution technique can be briefly described by the Fig. 3.

3. Case study

To evaluate the effectiveness of the model, an 8-hour time horizon discretized into a set of 1-minute periods is considered for the case study. The signal of frequency regulation from the grid is updated and the decisions of the aggregator are made at the beginning of each period. It is assumed that initially, there are 1000 EVs connected to the grid and controlled by the aggregator for the frequency regulation as shown in Fig. 4.

The EVs used in the case study are assumed from three different categories with different technological parameters (Battery University, 2016; Honda Media Website, 2010; Idaho National Laboratory, 2015; Plugincars, 2017) as shown in Table 3. The SOCs of these EVs are randomly generated between 20% and the battery capacities (MIT Electric Vehicle Team, 2008). In addition, the EVs that will be connected to the grid at the beginning of different periods throughout the decision horizon are randomly selected from these three major brands. The corresponding SOCs are also randomly generated between 20% and 100% of the battery capacities.

Recall that the number of EVs that will be connected to the grid at each period follows Poisson distribution. Parking pattern of EVs at different periods of the day is referred (Alonso, Amaris, Germain, & Galan, 2014) to identify the mean connection rates at each period t, λ_t. The approximate maximum number of newly connected EVs at period t, $\underline{Q}_t$, is obtained by setting 0.99 as the threshold value of the cumulative distribution function of the Poisson distribution. The mean of the connection duration of each EV (i.e., the estimated and reported connection duration) is randomly drawn from a normal distribution with mean of 20 min and standard deviation of 4 min.

The bonus rates of both actual energy provided upon the dispatch signal and capacity reservation in frequency regulation should be determined by the frequency regulation compensation mechanism set by utility companies, Regional Transmission Organizations, or Independent System Operators. However, through the survey with quite a few such organizations in the market, there still lacks a mature compensation mechanism particularly designed for frequency regulation using aggregated EVs. Therefore, in this case, the compensation mechanism using some quick-start and fast-ramp power systems in frequency regulation is referred. For example, PJM's frequency regulation service market has once offered \$40-\$50 per MWh for capacity plus actual energy provided since 2012 for quick-start and fast-ramp power from batteries and other load control systems (Walton, 2015). The rate is split to two parts, i.e., bonus rates of capacity reserved and actual energy provided following a 7:3 ratio. Thus, the bonus rates for the capacity reserved for frequency regulation in different periods are randomly drawn from the interval between \$0.028 and \$0.035 per

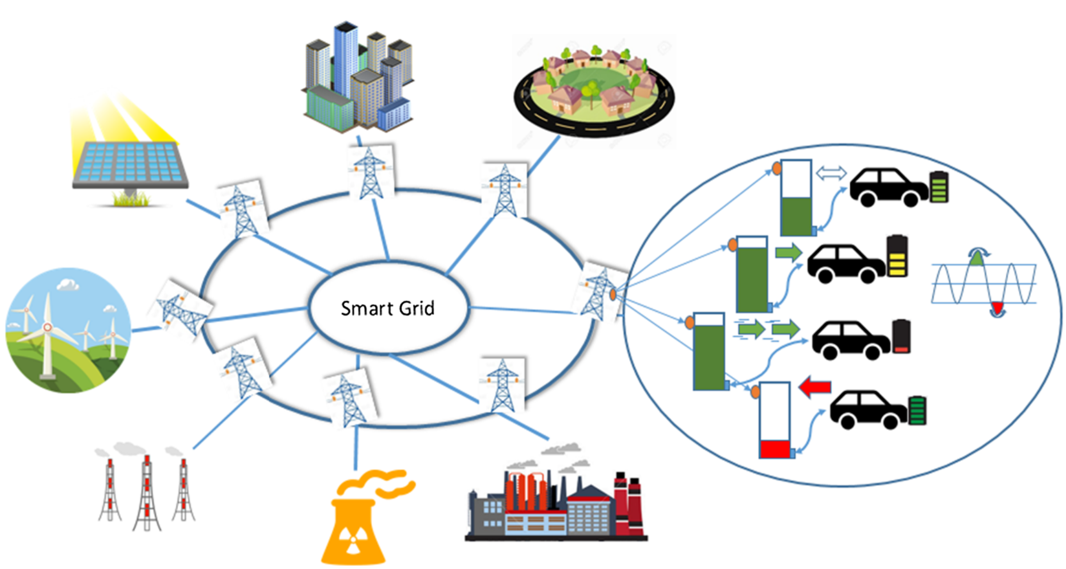

Fig. 4. EVs connected to the grid for the frequency regulation.

Table 3
Load characteristics of the three types of electric vehicles.

Type	Rated battery capacity (kWh)	Fast charging rate (kW)	Regular charging rate (kW)	Discharging rate (kW)
1	30	45	6.6	6.6
2	50	50	9.6	9.6
3	33	50	7.7	7.7

kWh. The bonus rates for the actual energy contribution for frequency regulation in different periods are randomly drawn from the interval between $0.012 and $0.015 per kWh.

The payment to the EV owners due to discharging depends on the degradation cost of unit energy discharged. In this case, $0.023 per kWh is set as the degradation payment rate for discharging referring to the model proposed by Shi, Xu, Wang, and Zhang (2017) and the general cell cost of the battery (Electrek, 2017). Further, the degradation cost of fast charging is set as $0.012 per kWh. The signals denoting either regulation up or down at each one-minute period are randomly generated.

After running the case with the proposed decision making model and solution strategy, the resultant action profiles of each group of EVs throughout the 8-hour horizon are obtained and shown in Fig. 5.

The actual contributions with respect to the variation of energy flow throughout the 8-hour horizon are shown in Fig. 6. The service level of the aggregated EVs is defined as the ratio between the number of periods during which the energy variation matches the desired regulation up/down signal and the total number of periods. In Fig. 4, the achieved service level is 84.02%.

The comparison of the revenue among the proposed semi-online solution strategy, the one-step ahead strategy, and the baseline heuristic strategy is shown in Table 4. The revenue obtained by the aggregator using the one-step ahead strategy is 8.3% higher than the baseline strategy, while the proposed solution strategy can increase the revenue approximately 15.09% compared to the baseline strategy.

Due to the concerns of battery degradation and the fact that there lack very mature compensation mechanisms in the frequency regulation market using aggregated EVs, the case is again investigated with possible higher bonus rates and degradation payment rates to examine the influence of the encouraging factor (compensation mechanism) and the discouraging factor (degradation payment rate) on the economic viability (the revenue) and service quality (service level) of the proposed model.

The higher bonus rates, i.e., the rates for reserved capacity and actual energy contribution are randomly drawn from the intervals between $0.032 and $0.035 as well as between $0.048 and $0.055, respectively, are considered. Also, the higher degradation cost rates due to discharging and fast charging, $0.083 per kWh, and $0.025 per kWh (Shi et al., 2017) are considered. Table 5 and Fig. 7 show the comparisons among the four different scenarios based on different bonus rates and degradation costs.

It is observed from Fig. 7 that there is no strong interaction between bonus rate and degradation cost rate in terms of the variation of the revenue. The increase of bonus rate will lead to the increase of aggregator's revenue disregarding the level of degradation cost rate, while the increase of degradation cost rate will lead to the decrease of aggregator's revenue at both levels of the bonus rates. These observations match the intuitive understanding according to the revenue function of the aggregator. More specifically, when increasing the bonus rate, the increase of the revenue at the higher degradation cost rate is a little bit larger than the lower degradation cost rate. Also, when increasing the degradation cost rate, the decrease of the revenue at the lower bonus rate is a little bit larger than the higher bonus rate.

However, as for the service level, the result is more interesting. Strong interactions exist between the bonus rate and the degradation cost rate. The variations of the service level due to the change of bonus rate (or degradation cost rate) are different when the degradation cost rate (or bonus rate) is at different levels. Intuitively, a higher bonus rate and lower degradation cost rate can encourage the aggregator to take more actions that can accommodate the desired direction of energy flow variation requested by grid signals to facilitate more participation and contribution from EVs, which seems to imply a higher service level. While a higher degradation rate may limit such an intention of aggregator to take actions as much as possible. The results illustrated in Table 5 are inverse to these intuitive understandings. It implies the necessity of designing an optimal pair of bonus rate and degradation cost rate that leads to a maximized service level.

In addition to the constant degradation payment rate, dynamic degradation payment rate is also examined to address the concern that a single EV may be discharged or fast charged for many times. A dynamic degradation payment is used where the payment at each time is equal to the times that EV is discharged or fast charged multiplying the base rate $0.023 per kWh and $0.025 per kWh, respectively. In other words, the payment is linearly proportional to the times that the EV has been discharged or fast charged. The distributions of the times of discharging and fast charging using constant and dynamic degradation rates are illustrated in Fig. 8. It can be seen that after adopting a dynamic degradation cost mechanism, the numbers of EVs that are discharged or fast charged are reduced.

The comparison of the revenue and service level between the constant and dynamic degradation payment mechanisms is shown in Table 6. The 95% confidence intervals of the revenue and service level of two degradation payment mechanisms are not overlapped, which indicates that there is a significant difference between two mechanisms. The revenue and the service level are decreased while applying the dynamic degradation cost rates. It is because the dynamic mechanism prefers to protect EV battery rather than provide service according to the frequency regulation signal requested by the grid. It limits the possibility of the occurrence of adoption of discharging and fast charging.

4. Discussion

4.1. Economic viability of frequency regulation using aggregated EVs

Since frequency regulation using aggregated EVs is an emerging idea, which has not yet been widely adopted, it is hard to find relevant data from the existing literature to estimate the overall cost and benefit as well to quantitatively and systematically compare the performance with respect to economic viability between the traditional regulation methods and the proposed method. When aggregated EVs are used in frequency regulation, the economic viability needs to be further analyzed, considering the interests from three involved parties: EV owners, aggregators, and grid & utility companies.

From the perspective of the EV owners, the major concern is the cost of battery degradation due to additional charging/discharging cycles in frequency regulation. The compensation payment has an impact on the participation willingness of the EV owners, which further influences the economic viability of the frequency regulation using EVs. Many studies focusing on the relationship between battery lifetime and working cycle have been reported. In this paper, the payment to the EV owners for this concern is quantified, considering general cell cost as well as a typical degradation model (Electrek, 2017; Shi et al., 2017) to cover the battery degradation cost. Furthermore, the additional revenue in grid service is also expected by the EV owners to partially offset the high cost when purchasing the EVs, especially EVs with the hardware modules to facilitate the bidirectional energy and information flow in frequency regulation. The lifetime operational savings of the EV owners who switched from regular fuel can be increased (Markel, Meintz, Hardy, Chen, Bohn, Smart, & Kiliccote, 2015), which can potentially boost future EV sales, and in turn, offer more available resources in frequency regulation.

From the perspective of the grid & utility companies, the economic viability depends on the cost of building the required infrastructure to facilitate the energy and information flow and to enable the coordination between the EVs and the grid. A few studies focused on the profitability analysis have been reported (Kempton & Tomic, 2005; Schuller & Rieger, 2013; Tomić & Kempton, 2007). For example, Kempton and Tomic (2005) concluded that V2G can be profitable to the grid and utility company for short term energy storage and is to some extent competitive with peak power generators for the grid. A further analysis by Tomić and Kempton (2007) investigated the economic viability of regulation services using fleets of EVs based on the study of four electric markets with different market clearing prices. They focused on the importance of market clearing price and illustrated a situation in which regulation service using EVs is not economically viable because of low market clearing prices for the regulation services using

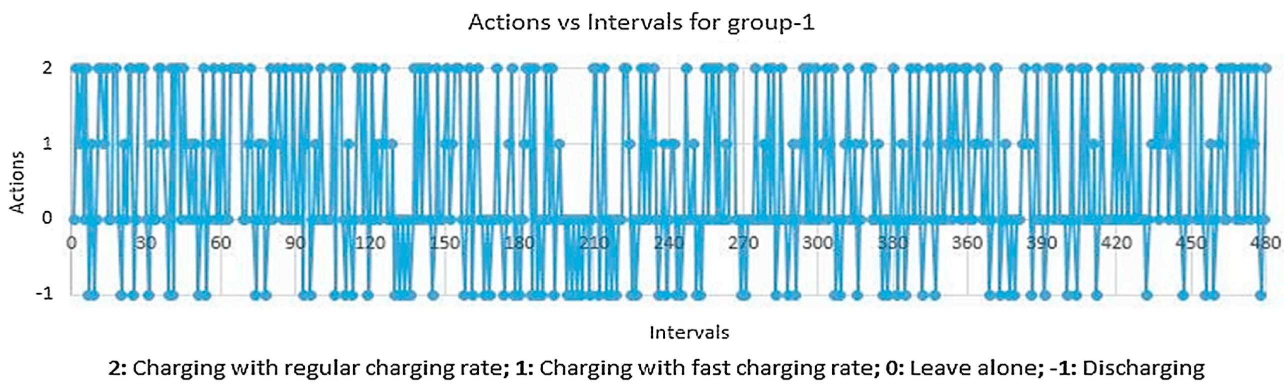

A. Action profile of group-1
(Chargeable with fast charging rate and dischargeable)

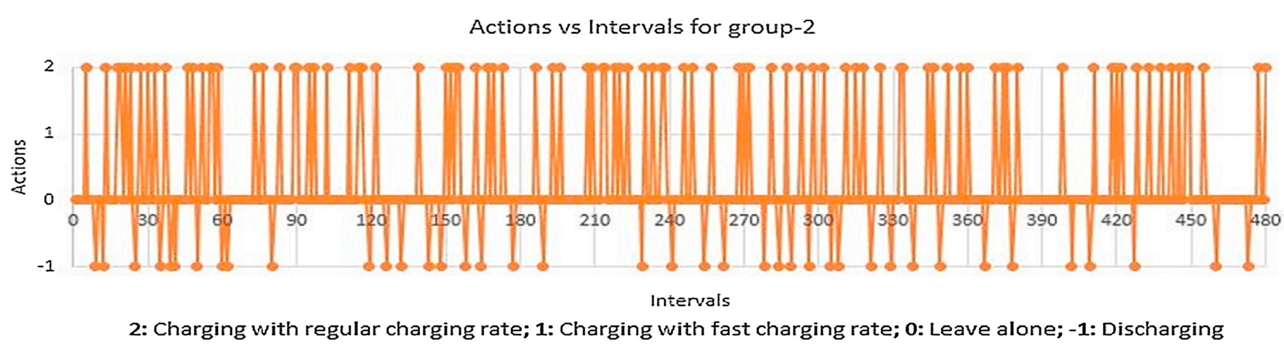

B. Action profile of group-2
(Chargeable with regular charging rate and dischargeable)

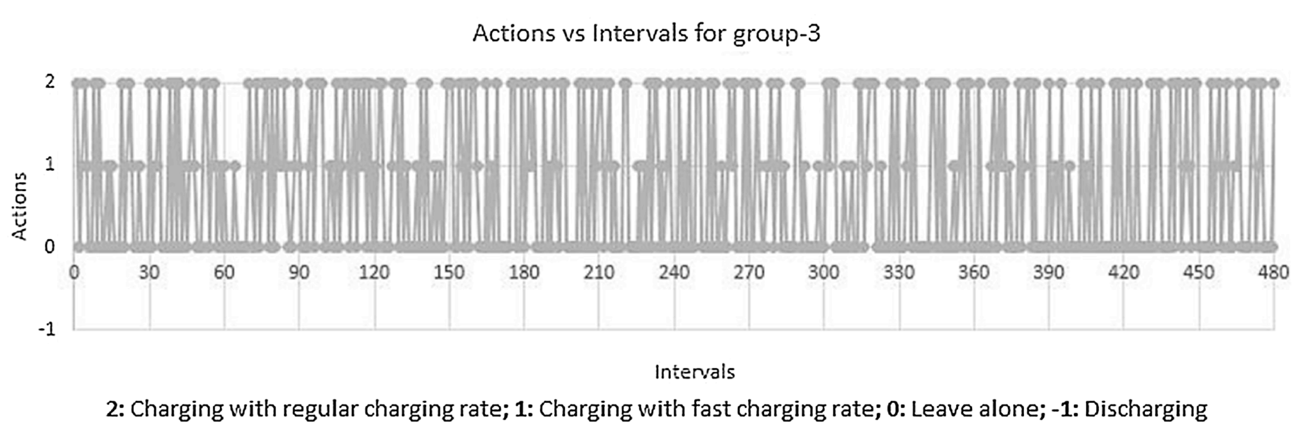

C. Action profile of group-3
(Chargeable with fast charging rate and not dischargeable)

Fig. 5. Action profiles of each group of EVs.

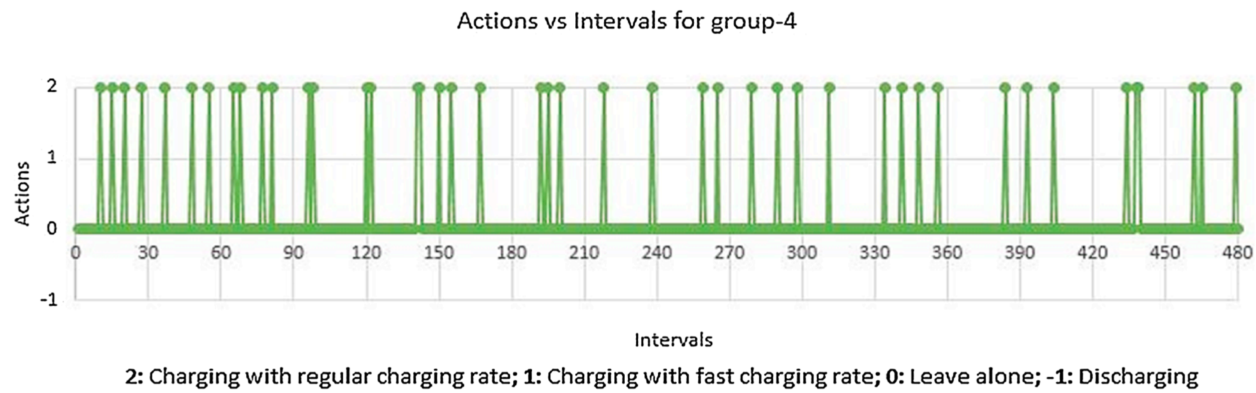

D. Action profile of group-4
(Chargeable only with regular charging rate and not dischargeable)

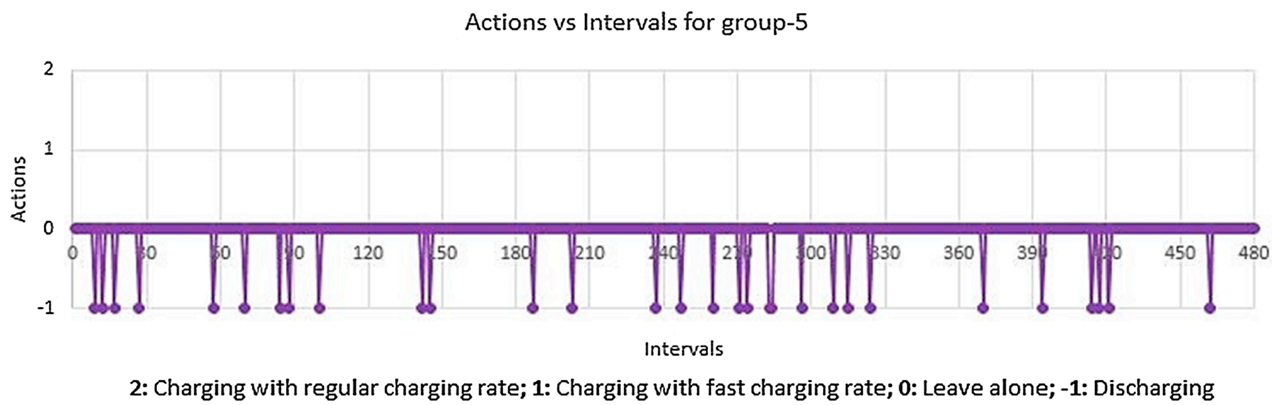

E . Action profile of group-5
(Dischargeable and not chargeable)

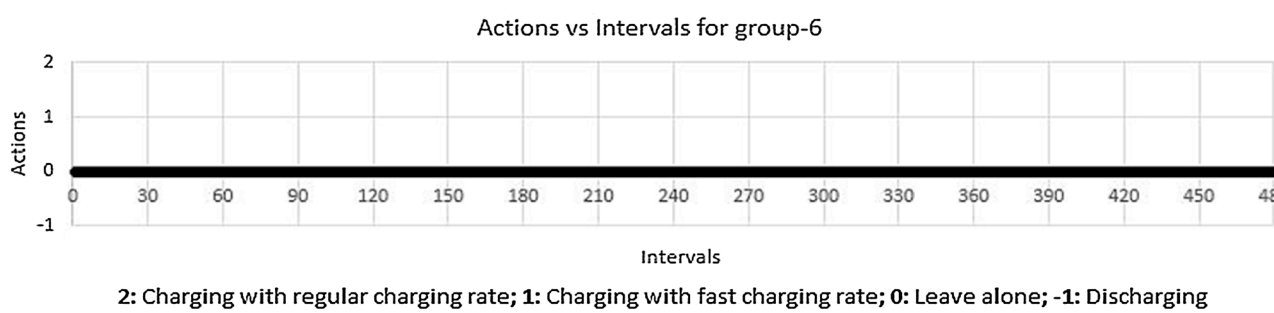

F. Action profile of group-6
(Neither chargeable nor dischargeable)

Fig. 5. (*continued*)

the generators. Schuller and Rieger (2013) conducted an economic evaluation of EVs participating in the ancillary service market (primary, secondary, and tertiary regulation) for the case of Germany and concluded that it was a profitable option to integrate EVs for ancillary service. They examined the economic potential of nine general options (based on positive and negative regulation) in the regulation market

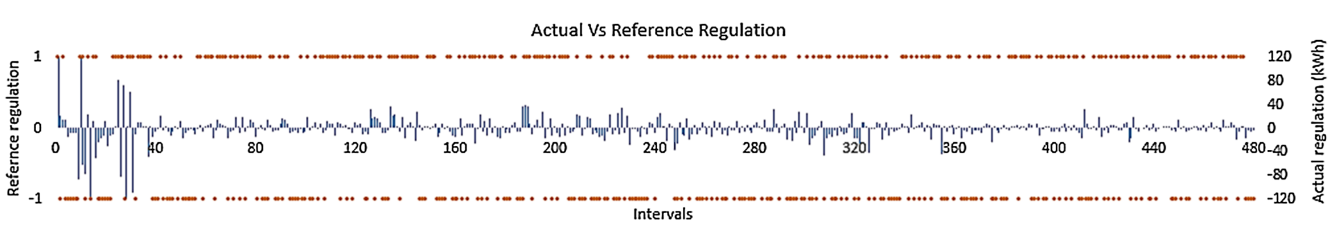

Fig. 6. Actual energy contribution.

Table 4
Comparison of revenue among the solution strategies.

	Proposed model	One-step ahead model	Baseline model
Mean revenue ($)	15209.08	14320.21	13214.80
95% C.I.	(14938.68, 15479.48)	(14151.63, 14458.8)	(13002.64, 13326.96)
Increase	15.09%	8.3%	

based on real-life EV specifications, connection powers, and regulation energy prices. However, there still lacks a systematic investigation that estimates the overall cost for building the required hardware infrastructure as well as the benefit of aggregated EVs being used in frequency regulation.

From the perspective of the EV aggregators, some studies with respect to the economic viability analysis have been reported (Capion, 2009; Pelzer, Ciechanowicz, Aydt, & Knoll, 2014; Sarker, Dvorkin, & Ortega-Vazquez, 2016). For example, Pelzer et al. (2014) developed a charging and dispatching strategy for optimizing the profits of the system aggregator in V2G integration. Capion (2009) developed a model that defines the optimal charging plan for EV fleets to minimize the total cost (fuel, electricity, and battery wear) for a system operator in Western Denmark. Sarker et al. (2016) proposed a bidding strategy for the aggregator to maximize its profit from participating in competitive energy and different regulating reserves markets, while compensating EV owners for battery degradation. These studies have focused on the economic viability analysis and modeling from the perspective of operation, ignoring the cost required for designing the system. It is required to develop an effective decision making algorithm for the energy flow control between the grid and the EVs and build the infrastructure to efficiently implement and control the charging/discharging scheme identified by the algorithm.

Therefore, the cost/benefit analysis for the stakeholders of the grid & utility companies, the EV aggregators, and the EV owners must be systematically analyzed and modeled. The possible conflicts between different parties needs to be carefully balanced using novel technologies to improve the overall economic viability of this grid service to all the stakeholders. The overall benefit to the system should be measured through a comparison considering the cost reduction due to the less use of traditional regulation sources and the additional cost to involve the aggregated EVs. The results of the case study show that the revenue of the aggregator (the income from both reservation and energy flow minus the cost of fast charging and discharging) is not trivial. The allocation of this revenue should be further investigated. For example, besides degradation payment, an additional bonus could be considered for the EV owners to offset the initial cost of purchasing EVs and to attract more participation. The revenue could also be scaled up by considering different sizes of aggregated EVs and different time horizons, which allows it to be discounted along the time horizon to estimate the maximum initial investment for the infrastructure while considering performance measures such as net present value, rate of return, etc.

4.2. Impact on battery lifespan

A major concern from the main contributor (i.e., EV owners) when providing the energy stored in the battery in frequency regulation is battery degradation. The existing literature has shown that the battery degradation is a nonlinear process with respect to the use time, and factors of degradation include depth of discharging, charging/discharging rate, ambient temperature, battery maintenance procedures, etc. (Drouilhet, Johnson, Drouilhet, & Johnson, 1997). Many degradation models have been developed to reveal the relationship between the degradation and some possible driven factors (Aurbach, Weissman, Yamin, & Elster, 1998; Guo & Fang, 2013; Shirk & Wishart, 2015; Xu, Oudalov, Ulbig, Andersson, & Kirschen, 2018). For example, Xu et al. (2018) showed that the capacity of the lithium-ion batteries is sensitive to both the number of working cycles and the depth of discharge of the cycle. Shirk and Wishart (2015) explored the impacts of fast charging on battery life and vehicle performance and observed a greater loss in capacity due to accelerated degradation because of fast charging. Aurbach et al. (1998) demonstrated the correlation between charge/discharge rates and morphology, surface chemistry, and performance of lithium-ion batteries and concluded that fast charging leads to a decrease in cycle life.

Generally, it has been recognized that fast charging, discharging, and depth of discharging have a profound effect on battery life. To compensate for the battery degradation and maintain the participation willingness of the EV owners, the degradation cost is considered in the model for both discharging and fast charging based on the degradation model proposed by Shi et al. (2017). In addition to the constant degradation payment rate, a dynamic degradation payment rate (where the payment is linearly proportional to the times that the EV has been discharged or fast charged) is also examined to address the concern that a single EV may be discharged or fast charged too many times. From the case study, it is observed that the dynamic degradation cost mechanism can drive the decision-making model to more widely utilize the available EV sources, reducing the possibility of over utilizing a certain small group of EVs.

5. Conclusion and future work

In this paper, a new computerized methodology for modeling and solving an industrial engineering problem is proposed to the targeted audience of researchers, educators, and practitioners of industrial engineering, especially in smart grid, and stochastic model of complex systems. The concerns of both the transportation sector and the power utility & grid industry are combined through an analytical decision-making model that integrates two novel technologies: EVs and smart grid. Markov decision process is used to model the decision-making procedure for frequency regulation using aggregated EVs from the perspective of an EV aggregator. A semi-online real-time solution strategy is proposed to identify the near-optimal decisions of frequency regulation for each EV. A numerical case study is implemented to demonstrate the usefulness of the proposed decision making model and

Table 5
Comparison of the revenue and service level among different scenarios.

Scenarios	Bonus	Degradation	Mean revenue ($)	95% C.I.	Mean service level (%)	95% C.I.
I	Low	Low	15209.08	(14938.68, 15479.48)	84.02%	(83.49%, 84.54%)
II	Low	High	13397.83	(13112.80, 13682.87)	77.88%	(77.17%, 78.59%)
III	High	High	15333.24	(15860.16, 16675.17)	84.15%	(82.98%, 85.32%)
IV	High	Low	16267.67	(14959.37, 15707.10)	75.18%	(74.74%, 75.63%)

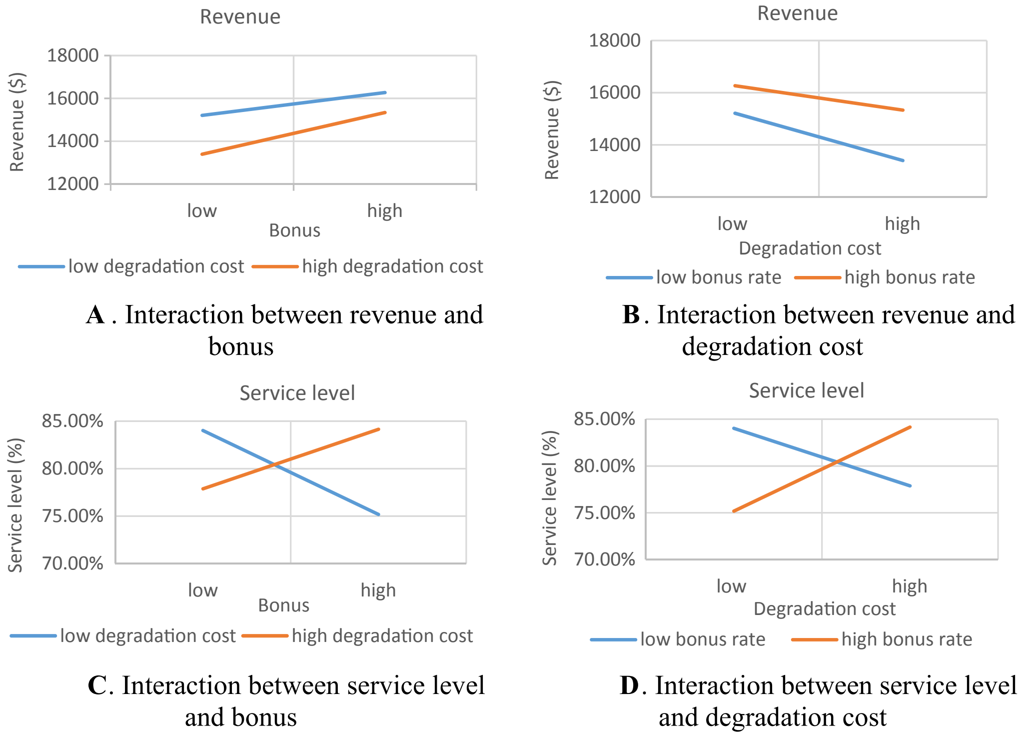

Fig. 7. Comparisons among the four different scenarios based on different bonus rate and degradation cost.

solution strategy.

The results of the case study show that the revenue gained by the EV aggregator is not trivial, which implies the potential economic viability of using aggregated EVs in frequency regulation. The allocation of the revenue obtained by the aggregator may be studied to design a more appealing incentive mechanism in order to further encourage EV owners to participate in the program. A systematic economic viability investigation considering the interests of the EV owners, the EV aggregators, and the grid & utility companies is needed to further clarify the feasibility and superiority of using aggregated EVs as a resource in

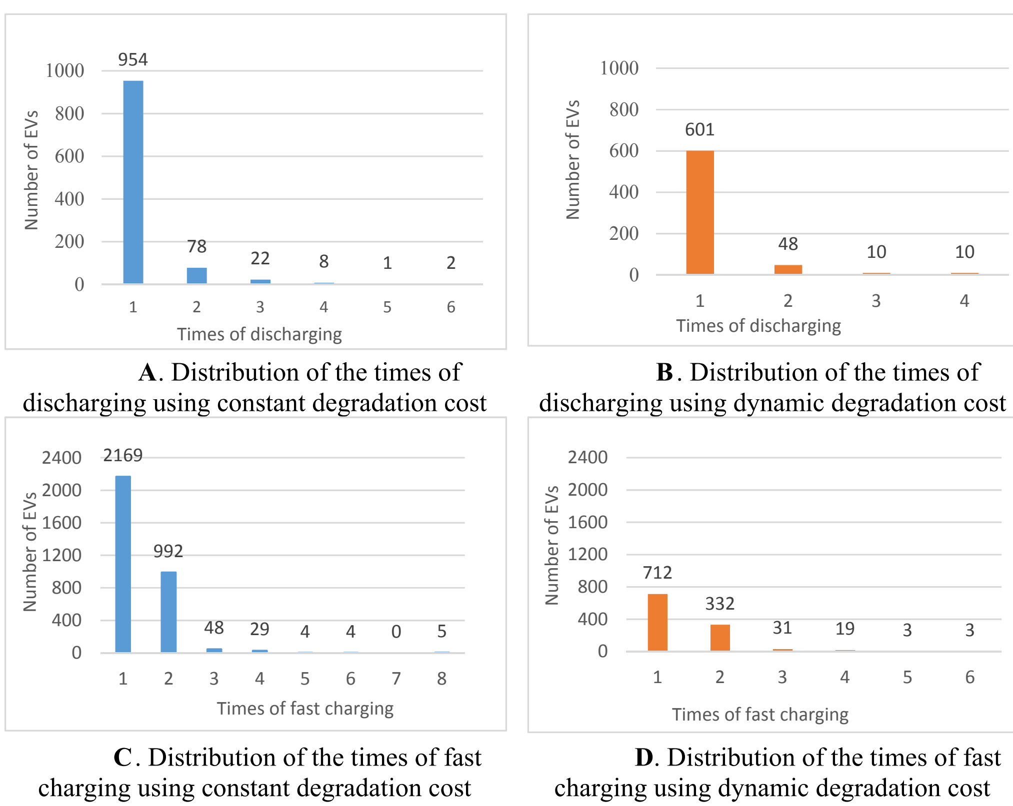

Fig. 8. Distribution of the times of discharging and fast charging using constant and dynamic degradation cost.

Table 6
Comparison of the revenue and service level due to constant and dynamic degradation cost.

	Constant	Dynamic
Average revenue ($)	15209.08	13605.15
Revenue, 95% C.I. ($)	(14938.68, 15479.48)	(13464.61, 13745.70)
Mean service level	84.02%	75.95%
Service level, 95% C.I.	(83.49%, 84.54%)	(74.88%, 77.02%)

frequency regulation compared to the existing traditional frequency regulation methods. The mixture of the different regulation sources including both aggregated EVs and other types of generators can also be studied.

In addition, the potential achievable contributions of frequency regulation are made by a given policy and given travel pattern of the aggregated EVs in the case study. Thus, future research may focus on estimating the effects of filling the gap between local generation and demand in frequency regulation while considering the travel patterns of the local EVs. Furthermore, the EVs parked at various venues (e.g., the airport parking lot, metro-station parking lot, office parking lot, etc.) with unique characteristics of the connection duration, can be fitted into the model. Also, more experiments on the price mechanism can be carried out using various designs to quantify the mathematical relationships between the revenue/service level and price mechanism so that the optimal price/incentive mechanism can be identified.

References

Alonso, M., Amaris, H., Germain, J. G., & Galan, J. M. (2014). Optimal charging scheduling of electric vehicles in smart grids by heuristic algorithms. *Energies, 7*, 2449–2475.

Aurbach, D., Weissman, I., Yamin, H., & Elster, E. (1998). The correlation between charge/discharge rates and morphology, surface chemistry, and performance of Li electrodes and the connection to cycle life of practical batteries. *Journal of The Electrochemical Society, 145*(5), 1421–1426.

Awasthi, A., & Omrani, H. (2019). A goal-oriented approach based on fuzzy axiomatic design for sustainable mobility project selection. *International Journal of Systems Science: Operations & Logistics, 6*(1), 86–98.

Battery University. (2016). BU-1003: Electric Vehicle (EV). Available online: < http://batteryuniversity.com/learn/article/electric_vehicle_ev > .

Bellman, R. (1957). *Dynamic programming.* Princeton, NJ: Princeton University Press.

Brooks, A. (2002). Vehicletogrid demonstration project: Grid regulation ancillary service with a battery electric vehicle. *AC Propulsion*.

Capion, K. (2009). *Optimized charging of electric drive vehicles in amarket environment. Master's Thesis.* Riso National Laboratory for Sustainable Energy and Technical University of Denmark.

Clement-Nyns, K., Haesen, E., & Driesen, J. (2010). The impact of charging plug-in hybrid electric vehicles on a residential distribution grid. *IEEE Transactions on Power Systems, 25*(1), 371–380.

Dallinger, D., Krampe, D., & Wietschel, M. (2011). Vehicle-to-grid regulation reserves based on a dynamic simulation of mobility behavior. *IEEE Transactions on Smart Grid, 2*(2), 302–313.

Drouilhet, S., Johnson, B., Drouilhet, S., & Johnson, B. (1997). A battery life prediction method for hybrid power applications. In 35th Aerospace Sciences Meeting and Exhibit (p. 948).

Du, S., Xu, R., Huang, D., & Yao, X. (2015). Markov modeling and analysis of multi-stage manufacturing systems with remote quality information feedback. *Computers & Industrial Engineering, 2015*(88), 13–25.

Duan, C., Deng, C., Gharaei, A., Wu, J., & Wang, B. (2018). Selective maintenance scheduling under stochastic maintenance quality with multiple maintenance actions. *International Journal of Production Research, 56*(23), 7160–7178.

Dubey, R., Gunasekaran, A., Sushil, & Singh, T. (2015). Building theory of sustainable manufacturing using total interpretive structural modelling. *International Journal of Systems Science: Operations & Logistics, 2*(4), 231–247.

Electrek. (2017). Electric vehicle battery cost dropped 80% in 6 years down to $227/kWh – Tesla claims to be below $190/kWh. Available online: < https://electrek.co/2017/01/30/electric-vehicle-battery-cost-dropped-80-6-years-227kwh-tesla-190kwh/ > .

EPRI (Electric Power Research Institute). (2007). Environmental assessment of plug-in hybrid electric vehicles. In Nationwide Greenhouse Gas Emissions, vol. 1, Electric Power Research Institute, Palo Alto.

European Union (2014). Energy Research and Challenges for Smart Cities. Available online: < https://setis.ec.europa.eu/energy-research/sites/default/files/library/ERKC_PB_Smart_Cities.pdf > .

Falahati, S., Taher, S. A., & Shahidehpour, M. (2016). A new smart charging method for EVs for frequency control of smart grid. *International Journal of Electrical Power & Energy Systems, 83*, 458–469.

FERC (Federal Energy Regulatory Commission). (2011). Frequency regulation compensation in the organized wholesale power markets, United States of America. 137 FERC: 61,064.

Fox Business. (2017). China sets new deadline for electric-car production. Available online: < http://www.foxbusiness.com/markets/2017/09/28/china-sets-new-deadline-for-electric-car-production.html > .

Gharaei, A., Hoseini Shekarabi, S. A., & Karimi, M. (2019). Modelling and optimal lot-sizing of the replenishments in constrained, multi-product and bi-objective EPQ models with defective products: Generalised Cross Decomposition. *International Journal of Systems Science: Operations & Logistics,* 1–13.

Gharaei, A., Karimi, M., & Hoseini Shekarabi, S. A. (2019a). An integrated multi-product, multi-buyer supply chain under penalty, green, and quality control polices and a vendor managed inventory with consignment stock agreement: The outer approximation with equality relaxation and augmented penalty algorithm. *Applied Mathematical Modelling, 69*, 223–254.

Gharaei, A., Karimi, M., & Hoseini Shekarabi, S. A. (2019b). Joint economic lot-sizing in multi-product multi-level integrated supply chains: Generalized benders decomposition. *International Journal of Systems Science: Operations & Logistics,* 1–17.

Guille, C., & Gross, G. (2009). A conceptual framework for the vehicle-to-grid (V2G) implementation. *Energy Policy, 37*, 4379–4390.

Guo, Y., & Fang, Y. (2013). Electricity cost saving strategy in data centers by using energy storage. *IEEE Transactions on Parallel and Distributed Systems, 24*(6), 1149–1160.

Han, S., Han, S. H., & Sezaki, K. (2010a). *Design of an optimal aggregator for vehicle-to-grid regulation service.* IEEE1–8.

Han, S., Han, S., & Sezaki, K. (2010b). Development of an optimal vehicle-to-grid aggregator for frequency regulation. *IEEE Transactions on Smart Grid, 1*(1), 65–72.

Han, S., Han, S., & Sezaki, K. (2011a). *Optimal control of the plug-in electric vehicles for V2G frequency regulation using quadratic programming.* IEEE1–6.

Han, S., Han, S., & Sezaki, K. (2011). Estimation of achievable power capacity from plug-in electric vehicles for V2G frequency regulation: Case studies for market participation. *IEEE Transactions on Smart Grid, 2*(4), 632–641.

Hoseini Shekarabi, S. A., Gharaei, A., & Karimi, M. (2018). Modelling and optimal lot-sizing of integrated multi-level multi-wholesaler supply chains under the shortage and limited warehouse space: Generalised outer approximation. *International Journal of Systems Science: Operations & Logistics,* 1–21.

Holley, P. (2017). Death of gas and diesel begins as GM announces plans for 'all-electric future'. Available online: < https://www.washingtonpost.com/news/innovations/wp/2017/10/02/death-of-diesel-begins-as-gm-announces-plans-for-all-electric-future/ > .

Honda Media Website. (2010). Honda to start electric vehicle testing program with Saitama prefecture: Honda's next-generation personal mobility test vehicles and charging facilities make public debut. Available online: < http://www.hondanews.info/news/en/auto/4101220aeng? > .

Hao, Y., Helo, P., & Shamsuzzoha, A. (2018). Virtual factory system design and implementation: Integrated sustainable manufacturing. *International Journal of Systems Science: Operations & Logistics, 5*(2), 116–132.

Huang, Z. J., & Ma, J. (2011). Solving the curse of dimensionality utilizing action-dependent heuristic dynamic programming. In Proceedings of computer science and automation engineering (CSAE), IEEE international conference, Shanghai, China, June 10–12, 2011, vol. 2, pp. 289–92.

Idaho National Laboratory. (2015). Steady state vehicle charging fact sheet: 2015 Nissan Leaf. Available online: < https://avt.inl.gov/sites/default/files/pdf/fsev/SteadyStateLoadCharacterization2015Leaf.pdf > .

Islam, M.M., Sun, Z., & Qin, R. (2018). Simulation-based investigation on economic feasibility of frequency regulation using aggregated electric vehicles in smart grid. In proceedings of IISE 2018 Annual Conference, May, 2018, Orlando, FL, U.S.

Izadkhast, S., Garcia-Gonzalez, P., & Frías, P. (2015). An aggregate model of plug-in electric vehicles for primary frequency control. *IEEE Transactions on Power Systems, 30*(3), 1475–1482.

Jian, M. E. N. G., Yunfei, M. U., Jianzhong, W. U., Hongjie, J. I. A., Qian, D. A. I., & Xiaodan, Y. U. (2015). Dynamic frequency response from electric vehicles in the Great Britain power system. *Journal of Modern Power Systems and Clean Energy, 3*(2), 203–211.

Jin, C., Tang, J., & Ghosh, P. (2013). Optimizing electric vehicle charging: A customer's perspective. *IEEE Transactions on Vehicular Technology, 62*(7), 2919–2927.

Kazemi, N., Abdul-Rashid, S. H., Ghazilla, R. A. R., Shekarian, E., & Zanoni, S. (2018). Economic order quantity models for items with imperfect quality and emission considerations. *International Journal of Systems Science: Operations & Logistics, 5*(2), 99–115.

Kempton, W., & Dhanju, A. (2006). Electric vehicles with V2G: Storage for large-scale wind power. *Windtech International, 2*(2), 18–21.

Kempton, W., & Tomic, J. (2005). Vehicle-to-grid power fundamentals: Calculating capacity and net revenue. *Journal of Power Sources, 144*(1), 268–279.

Kempton, W., Tomic, J., Letendre, S., Brooks, A., & Lipman, T. (2001). Vehicle-to-grid power: Battery, hybrid, and fuel cell vehicles as resources for distributed electric power in California CARB, CEPA, LA Dept. Water and Power, Electric Transportation Program.

Kempton, W., Udo, V., Huber, K., Komara, K., Letendre, S., Baker, S., …, Pearre, N. (2008). A test of vehicle-to-grid (V2G) for energy storage and frequency regulation in the PJM system, Univ. Delaware, Newark, DE.

Ko, Y. D., Jang, Y. J., & Lee, M. S. (2015). The optimal economic design of the wireless powered intelligent transportation system using genetic algorithm considering nonlinear cost function. *Computers & Industrial Engineering, 89*, 67–79.

Li, L., & Sun, Z. (2013). Dynamic energy control for energy efficiency improvement of sustainable manufacturing systems using Markov decision process. *IEEE Transactions on Systems, Man, and Cybernetics: Systems, 43*(5), 1195–1205.

Li, L., Sun, Z., Yang, H., & Gu, F. (2012). Simulation-based energy efficiency improvement for sustainable manufacturing systems. In Proceedings of ASME 2012 international manufacturing science and engineering conference collocated with the 40th North American manufacturing research conference and in participation with the international conference on tribology materials and processing (pp. 1033–1039), Notre Dame, Indiana, USA, June 4–8, 2012.

Liu, C., Chau, K. T., & Wu, D. (2013). Opportunities and challenges of vehicle-to-home, vehicle-to-vehicle, and vehicle-to-grid technologies, Invited paper, Vol. 101, No. 11, November 2013 Proceedings of the IEEE.

Liu, C., Huang, W., & Yang, C. (2017). The evolutionary dynamics of China's electric vehicle industry–Taxes vs. subsidies. *Computers & Industrial Engineering, 113*, 103–122.

Liu, R., Dow, L., & Liu, E. (2011). A survey of PEV impacts on electric utilities. In Proceedings of innovative smart grid technologies, IEEE PES, p. 1–8.

Lutsey, N. (2015). Global milestone: The first million electric vehicles. Available online: < http://www.theicct.org/blogs/staff/global-milestone-first-million-electric-vehicles > .

Markel, T., Meintz, A., Hardy, K., Chen, B., Bohn, T., Smart, J., … & Kiliccote, S. (2015). Multi-lab EV smart grid integration requirements study. Providing guidance on technology development and demonstration (No. NREL/TP-5400-63963). National Renewable Energy Lab.(NREL), Golden, CO (United States).

MIT Electric Vehicle Team (2008). A guide to understanding battery specifications. Available online: < http://web.mit.edu/evt/summary_battery_specifications.pdf > .

Nezamoddini, N., & Wang, Y. (2017). Real-time electricity pricing for industrial customers: Survey and case studies in the United States. *Applied Energy, 195*, 1023–1037.

Ortega-Vazquez, M. A., Kintner-Meyer, M. (2015). Electric vehicles and the electric grid, handbook of clean energy systems, Online©2015. John Wiley & Sons, Ltd.

Ortega-Vazquez, M. A., Bouffard, F., & Silva, V. (2013). Electric vehicle aggregator/system operator coordination for charging scheduling and services procurement. *IEEE Transactions on Power Systems, 28*(2), 1806–1815.

Pahasa, J., & Ngamroo, I. (2015). PHEVs bidirectional charging/discharging and SoC control for microgrid frequency stabilization using multiple MPC. *IEEE Transactions on Smart Grid, 6*(2), 526–533.

Pelzer, D., Ciechanowicz, D., Aydt, H., & Knoll, A. (2014). A price-responsive dispatching strategy for Vehicle-to-Grid: An economic evaluation applied to the case of Singapore. *Journal of Power Sources, 256*, 345–353.

Plugincars. (2017). BMW i3 Review-Small lightweight cutting-edge electric car. Available online: < http://plugincars.com/bmw-i3.html > .

Powell, W. B. (2007). *Approximate dynamic programming.* Hoboken, NJ: John Wiley & Sons2007.

Rabbani, M., Hosseini-Mokhallesun, S. A. A., Ordibazar, A. H., & Farrokhi-Asl, H. (2018). A hybrid robust possibilistic approach for a sustainable supply chain location-allocation network design. *International Journal of Systems Science: Operations & Logistics,* 1–16.

Rabbani, M., Foroozesh, N., Mousavi, S. M., & Farrokhi-Asl, H. (2019). Sustainable supplier selection by a new decision model based on interval-valued fuzzy sets and possibilistic statistical reference point systems under uncertainty. *International Journal of Systems Science: Operations & Logistics, 6*(2), 162–178.

Reuters. (2018). U.S. vehicle fuel economy rises to record 24.7 mpg: EPA. Available: < https://www.reuters.com/article/us-autos-emissions/u-s-vehicle-fuel-economy-rises-to-record-24-7-mpg-epa-idUSKBN1F02BX > .

Richardson, D. B. (2013). Electric vehicles and the electric grid: A review of modeling approaches, impacts, and renewable energy integration. *Renewable and Sustainable Energy Reviews, 19*, 247–254.

Roberts, D. (2017). The world's largest car market just announced an imminent end to gas and diesel cars. Available online: < https://www.vox.com/energy-and-environment/2017/9/13/16293258/ev-revolution > .

Rotering, N., & Ilic, M. (2011). Optimal charge control of plug-in hybrid electric vehicles in deregulated electricity markets. *IEEE Transactions on Power Systems, 26*(3), 1021–1029.

Sarker, M. R., Dvorkin, Y., & Ortega-Vazquez, M. A. (2016). Optimal participation of an electric vehicle aggregator in day-ahead energy and reserve markets. *IEEE Transactions on Power Systems, 31*(5), 3506–3515.

Sayyadi, R., & Awasthi, A. (2018a). A simulation-based optimisation approach for identifying key determinants for sustainable transportation planning. *International Journal of Systems Science: Operations & Logistics, 5*(2), 161–174.

Sayyadi, R., & Awasthi, A. (2018b). An integrated approach based on system dynamics and ANP for evaluating sustainable transportation policies. *International Journal of Systems Science: Operations & Logistics,* 1–10.

Schuller, A., & Rieger, F. (2013). Assessing the economic potential of electric vehicles to provide ancillary services: The case of Germany. *Zeitschrift für Energiewirtschaft, 37*(3), 177–194.

Shi, Y., Xu, B., Wang, D., & Zhang, B. (2017). Using battery storage for peak shaving and frequency regulation: Joint optimization for superlinear gains. Accepted by IEEE transactions on power systems. 10.1109/TPWRS.2017.2749512.

Shimizu, K., Masuta, T., Ota, Y., & Yokoyama, A. (2011). A new load frequency control method in power system using vehicle-to-grid system considering users' convenience. In Proc. 17th Power Syst. Comput. Conf. (pp. 1–7).

Shirk, M., & Wishart, J. (2015). Effects of electric vehicle fast charging on battery life and vehicle performance (No. INL/CON-14-33490). Idaho National Lab.(INL), Idaho Falls, ID (United States).

Sortomme, E., & El-Sharkawi, M. A. (2011). Optimal charging strategies for unidirectional vehicle-to-grid. *IEEE Transactions on Smart Grid, 2*(1), 131–138.

Sovacool, B. K., & Hirsh, R. F. (2009). Beyond batteries: An examination of the benefits and barriers to plug-in hybrid electric vehicles (PHEVs) and a vehicle-to-grid (V2G) transition. *Energy Policy, 37*, 1095–1103.

Steven Loveday. (2018). What is MPGe, U.S. News. Available: < https://cars.usnews.com/cars-trucks/what-is-mpge > .

Tomić, J., & Kempton, W. (2007). Using fleets of electric-drive vehicles for grid support. *Journal of Power Sources, 168*(2), 459–468.

Tsao, Y. C. (2015). Design of a carbon-efficient supply-chain network under trade credits. *International Journal of Systems Science: Operations & Logistics, 2*(3), 177–186.

U.S. EIA. (2018). Average quality of fossil fuel receipts for the electric power industry. Available: < https://www.eia.gov/electricity/annual/html/epa_07_03.html > .

U.S. EPA. (2018). Greenhouse gases equivalencies calculator – calculations and references. Available: < https://www.epa.gov/energy/greenhouse-gases-equivalencies-calculator-calculations-and-references > .

Vahedipour-Dahraie, M., Rashidizaheh-Kermani, H., Najafi, H. R., Anvari-Moghaddam, A., & Guerrero, J. M. (2017). Coordination of EVs participation for load frequency control in isolated microgrids. *Applied Sciences, 7*(6), 539.

Walton. (2015). Duke developing 2 MW storage facility for PJM frequency regulation. Available online: < http://www.utilitydive.com/news/duke-developing-2-mw-storage-facility-for-pjm-frequency-regulation/399802/ > .

Xia, T., Xi, L., Du, S., Xiao, L., & Pan, E. (2017). Energy-oriented maintenance decision-making for sustainable manufacturing based on MAM-ESW methodology. *Accepted by Journal of Manufacturing Science and Engineering.* https://doi.org/10.1115/1.4038996.

Xia, T., Xi, L., Zhou, X., & Du, S. (2012). Modeling and optimizing maintenance schedule for energy systems subject to degradation. *Computers & Industrial Engineering, 63*(3), 607–614.

Xu, B., Oudalov, A., Ulbig, A., Andersson, G., & Kirschen, D. S. (2018). Modeling of lithium-ion battery degradation for cell life assessment. *IEEE Transactions on Smart Grid, 9*(2), 1131–1140.

You, P. S., & Hsieh, Y. C. (2014). A hybrid heuristic approach to the problem of the location of vehicle charging stations. *Computers & Industrial Engineering, 70*, 195–204.

Zhang, A., Sun, B., Liu, T., Tan, X., Wang, S., & Tsang, D. H. (2018). Joint voltage and frequency regulation by EV charging scheduling in the distribution network. In 2018 IEEE power & energy society innovative smart grid technologies conference (ISGT) (pp. 1–5). IEEE.